DEVELOPING FORWARD MATHEMATICAL MODELS FOR SEABED LOGGING USING COMSOL

By

MUHAMMAD RIDHWAN BIN OTHMAN ZAKI

FINAL REPORT

Submitted to Electrical and Electronics Engineering Program

in Partial Fulfillment and Requirements

for the Degree

Bachelor of Engineering (Hons)

(Electrical and Electronics Engineering)

Universiti Teknologi Petronas

Bandar Seri Iskandar

31750 Tronoh

Perak Darul Ridzuan

CERTIFICATION OF APPROVAL

DEVELOPING FORWARD MATHEMATICAL MODEL FOR SEABED LOGGING USING COMSOL

by

Muhammad Ridhwan Bin Othman Zaki

A project dissertation submitted to the
Electrical & Electronics Engineering Programme
Universiti Teknologi PETRONAS
in partial fulfilment of the requirement for the
Bachelor of Engineering (Hons)
(Electrical & Electronics Engineering)

Approved:

_____
(Dr Afza bt Shafie)
Project Supervisor

Co-Supervisor
Puan Hanita Daud
Dr Zuhairi Baharudin

UNIVERSITI TEKNOLOGI PETRONAS
TRONOH, PERAK
July 2012

CERTIFICATION OF ORIGINALITY

This is to certify that I am responsible for the work submitted in this project, that the original work is my own except as specified in the references and acknowledgements, and that the original work contained herein have not been undertaken or done by unspecified sources or persons.

_____

(Muhammad Ridhwan Bin Othman Zaki)

ABSTRACT

Hydrocarbon exploration or known as oil and gas exploration is the search by petroleum geologist for hydrocarbon deposits beneath the Earth's surface such as oil and gas. Hydrocarbon exploration is needed before drilling to locate the location of the hydrocarbon. At sea level, there are various methods used for hydrocarbon exploration which are Seismic and Control Source Electromagnetic (CSEM) methods. Seismic method is using sound waves to explore geological structures underneath seabed in search for hydrocarbon. There are two types of seismic method which are refraction and reflection method. Both techniques are used in pair to visualize the earth structure. However, there is a problem using the seismic method which is the method cannot differentiate between the water, hydrocarbon and sediments. In order to overcome the problem, Seabed Logging is introduced. Seabed Logging (SBL) is a technique that utilizes the use of Electromagnetic (EM) waves. The EM waves from the antenna will propagate signals to reservoir depths where the difference in resistivity levels of different regions under the seafloor will help to determine possible oil wells for future exploration. Even though SBL is more preferable than Seismic because of its ability to differentiate between the water, hydrocarbon and sediments, the cost factor is the main reason why SBL is used as a compliment to Seismic Method. Exploring for hydrocarbon is also risky as anything can happen during the exploration. Therefore, the purpose of this project is to is to construct a 3D seabed model that later will be used to develop a forward mathematical method that can be used to determine the depths of the reservoir using different kind of frequencies.

TABLE OF CONTENTS

LIST OF FIGURES

LIST OF TABLES

LIST OF ABBREVIATION

SBL	Seabed Logging
EM	Electromagnetic
CSEM	Controlled Source Electromagnetic
MT	Magnetotelluric
HED	Horizontal Electric Dipole
FDTD	Finite Difference Time Domain
FDFD	Finite Difference Frequency Domain
FEM	Finite Element Method
MoM	Method of Moments
PDE	Partial Differential Equation

CHAPTER 1
INTRODUCTION

1.1 Background Study

Since 1970, seismic method is widely used for locating the hydrocarbon reservoir beneath the seabed. However, there is some disadvantage of using this method, seismic method is not able to differentiate the presences of water or hydrocarbon in the traps as the sound waves generate will only reflect if there is rock layers beneath the seafloor [1].

As a solution, research had been done; new technique named Seabed Logging (SBL) had been introduced to detect the location of the reservoir based on the hydrocarbon resistivity. Seabed logging applies the principle of Controlled Source Electromagnetic (CSEM) technology. The basis of the approach is the use of a mobile horizontal electric dipole (HED) source and an array of seafloor electric field receivers [1].

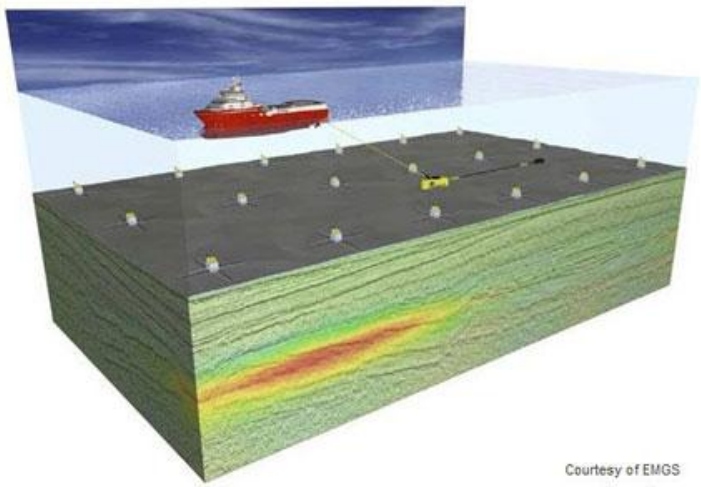

Figure 1: Seabed Logging

The transmitter is towed using a boat across the sensor (receiver) at the seabed. The source broadcast a controlled EM energy signal. Areas with high electric resistivity will reflect the electric current which later been recorded by the receiver for data

processing and analysis to indicate the presence of water or petroleum in underlying reservoir [2].

1.2 Problem Statement

There are 2 main problems that will be focused in this project:

i. SBL technology generates huge amount of unprocessed data which may not be interpreted directly.
ii. Present technique of processing the acquired data involve complicated mathematical modeling techniques such as Finite Element Method, Finite Integral Method, Finite Difference Method and etc.

1.3 Objectives

Objective of the project is to develop a forward mathematical model that relates depth of hydrocarbon with frequency. A 3D model of seabed logging will be developed using COMSOL software and the generated synthesis data will be processed using mathematical tools to generate the mathematical models.

1.4 Scope of Study

1.4.1 Understanding Seabed Logging

- A research will be done to have better understanding about the theoretical background for seabed logging and how seabed logging is done.
- A research also will cover on the measurement principle of seabed logging.
- There also minor research on the previous method which is seismic method to differentiate both techniques.

1.4.2 Using COMSOL to Generate Seabed Logging

- It is a need to install COMSOL on user's personal computer

- Minimum requirement for installation also need to be considered to have smooth operation in generating Seabed Model.
- Some research and training will be done to have basic idea on how to use the software
- After modeling the seabed model, the simulator will be used to model EM waves to detect the hydrocarbon using different variable. There are two variables to be concerned which are the depths and the frequencies.

1.5 Feasibility of Project

Students are given two semesters to complete the project. In first semester, author will focus on the research of Seabed Logging. The research will include how seabed logging works, the measurement principles and the different of seabed logging method and other method. The study will also focus on some idea on electromagnetic waves and how to use the software to develop the simulator.

For second semester, the focus will be more on data collection and interpretation. The data will then be used to develop forward mathematical model based on the relationship between the depths of the hydrocarbon and the frequencies of the waves.

With the resources available in University, the project is estimated to complete within this two semesters.

CHAPTER 2
LITERATURE REVIEW

2.1 Introduction

Detecting and assessing hydrocarbon reservoir without the need to drill test wells is the major important to petroleum engineering. Lots of studies and research had been done to develop new technique for the remote and direct identification of hydrocarbon reservoir in deep water areas. Previously, seismic method is widely used in hydrocarbon exploration but as it is not able to differentiate the presence of water or hydrocarbon in traps, seabed logging technique is preferable as it can cut cost and has better precision in hydrocarbon detection.

2.2 Seismic Exploration Method

During previous time, seismic methods have been used in hydrocarbon exploration. Seismic method uses sound waves to exploring geological structures underneath seabed in search for hydrocarbon. Computers are used to identify different rock layers and structures by calculating intensity of the reflected sound waves and the distances are calculated based on the time for the waves to travel through the rocks and back to the receivers. The data is used to create two or three-dimensional images of the layers and the location of these structures [3]. There are two techniques for seismic exploration method which are reflection and refraction technique which will be discussed on the next subtopic. Roughly, reflection method is used to define the depth of the potential reservoir while refraction method is used to identify the area of possible reservoir.

2.2.1 Seismic Refraction

Seismic refraction involves measuring the travel time of the component of seismic energy which travels down to the top of rock (or other distinct density contrast), is refracted along the top of rock, and returns to the surface as a head wave along a wave front similar to the bow wake of a ship (see **Figure 2**). The shock waves which return from the top of rock are refracted waves, and for geophones at a distance from the shot point, always represent the first arrival of seismic energy [4].

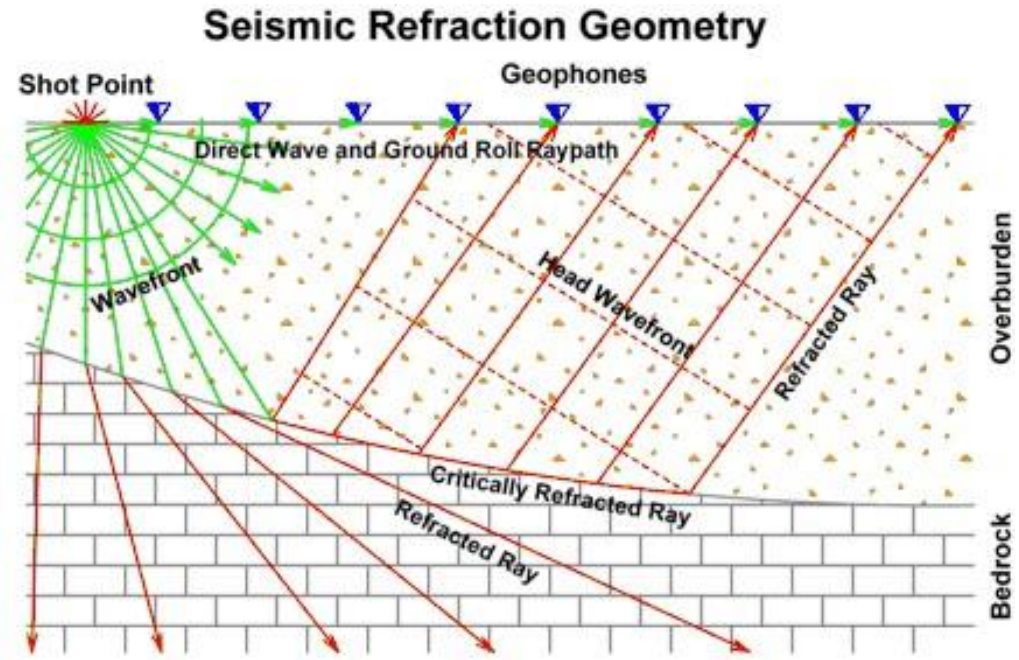

Figure 2: Seismic Refraction Geometry

2.2.2 Seismic Reflection

Seismic reflection uses field equipment similar to seismic refraction, but field and data processing procedures are employed to maximize the energy reflected along near vertical ray paths by subsurface density contrasts (see **Figure 3**). Reflected seismic energy is never a first arrival, and therefore must be identified in a generally complex set of overlapping seismic arrivals - generally by collecting and filtering multi-fold or highly redundant data from numerous shot points per geophone placement. The main limitations to seismic reflection are its higher cost than refraction (for sites where either

technique could be applied), and its practical limitation to depths generally greater than approximately 50 feet [4].

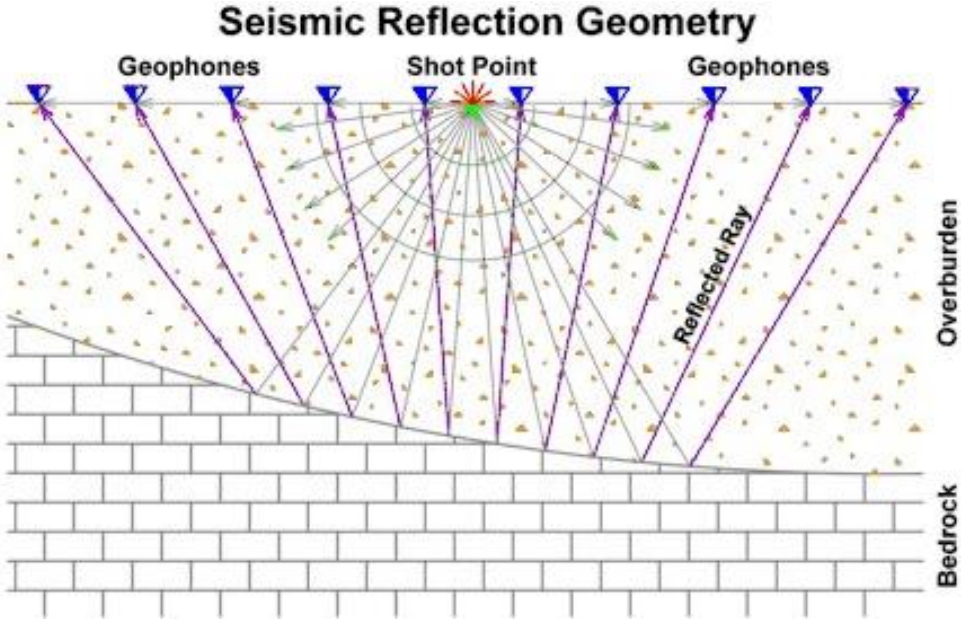

Figure 3: Seismic Reflection Geometry

2.3 Electromagnetic Geophysical Method

EM methods help the explorations by measuring the flow of electrical energy passing through the earth which allows us to identify conductor and resistor rocks [5]. The objective of electromagnetic (EM) geophysical method is to determine the electrical properties (conductivity, permittivity, and susceptibility) of the subsurface. Fluids like oil and gas has their own electrical conductivity which are lower than brines and water. Therefore, EM method can be used to differentiate between different types of offshore fluids based on their resistivity. Just as in seismic exploration, EM geophysics can contribute to hydrocarbon exploration in two distinct ways. Most often, EM methods are used to image structure that could host potential reservoirs and/or source rocks. In certain cases, they may also give evidence for direct indication of the presence of hydrocarbons. In hydrocarbon exploration since the cost for EM is high, the method is used as a complement with seismic method as the data provided by the seismic method cannot

exploit the differences between a reservoir containing highly resistive hydrocarbons and one saturated with conductive saline fluids.

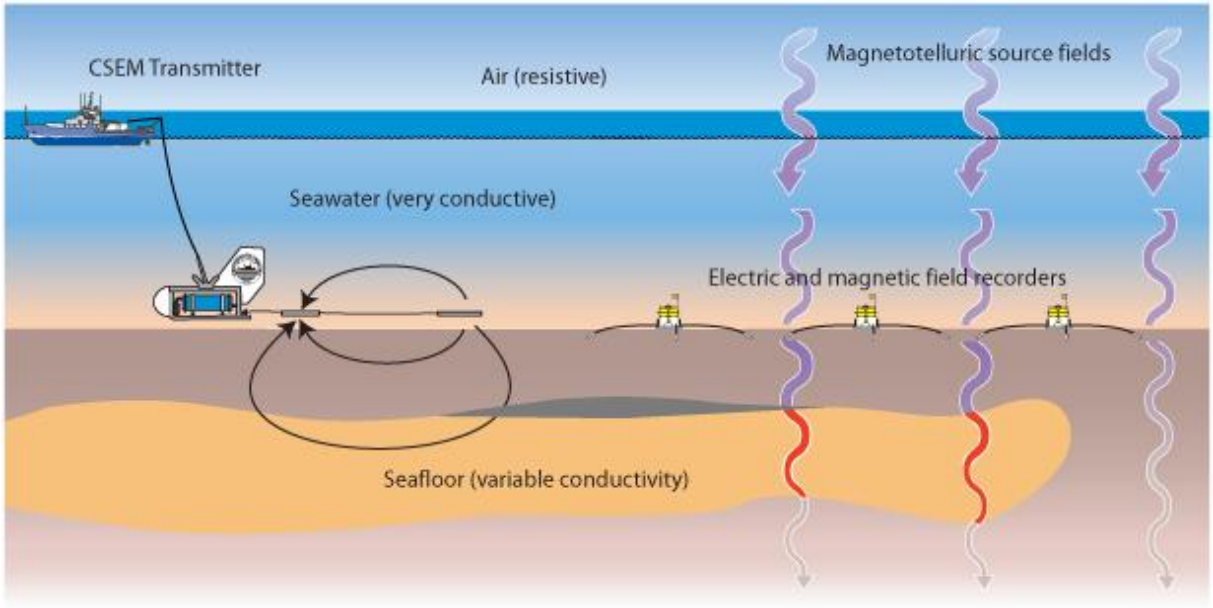

Figure 4: Concept Diagram for the Marine Controlled Source EM (CSEM) and Marine Magnetotelluric (MT) Method

2.3.1 Magnetotelluric (MT)

Magnetotellurics is a geophysical method that measures magnetic and electric fields that are found in the earth. Basically, Magnetotellurics is a geophysical method that measures naturally occurring, time-varying magnetic and electric fields [6]. Magnetotellurics uses natural, low frequency electromagnetic (EM) waves to image the subsurface. These waves have frequencies in the band 1000-0.0001 Hz and originate in worldwide lightning activity and oscillations of the magnetosphere (Vozoff, 1991). These electromagnetic signals travel through the atmosphere as radio waves but diffuse into the Earth and attenuate rapidly with depth.

In hydrocarbon exploration, Magnetotellurics method has been used to map sedimentary structure as an aid to petroleum exploration. The essence of the MT method

is the computation of electromagnetic earth impedance from measurements of orthogonal horizontal magnetic and electric fields at the surface. Estimates of impedance magnitude (transformed to an apparent resistivity) and phase at various frequencies allow investigation of electrical conductivity as a function of depth. Impedance measured at several locations allows investigation of conductivity as a function of horizontal position [7]. The resistivity distribution based on the low frequency of MT is then interpreted in terms of rock type and geologic structure [8].

2.3.2 Controlled Source Electromagnetic (CSEM)

Marine controlled-source electromagnetic (CSEM) surveying has been in commercial use for predrill reservoir appraisal and hydrocarbon exploration for 10 years. Although a recent decrease has occurred in the number of surveys and publications associated with this technique, the method has become firmly established as an important geophysical tool in the offshore environment [9]. This is a consequence of two important aspects associated with the physics of the method:

- It is sensitive to high electrical resistivity, which, although not an unambiguous indicator of hydrocarbons, is an important property of economically viable reservoirs.
- Although the method lacks the resolution of seismic wave propagation, it has a much better intrinsic resolution than potential-field methods such as gravity and magnetic surveying, which until now have been the primary non-seismic data sets used in offshore exploration.

The marine CSEM method operates best in deep water (more so than MT), and the rise in CSEM exploration coincides with the ability to produce hydrocarbons in water depths greater than 1000 m. The high cost of deep water drilling also supported the use of a relatively expensive non-seismic method [9]. CSEM method measures electromagnetic fields with sensors on the ocean floor. A deep-towed transmitting antenna then generates low-frequency electromagnetic fields, which later be detected by the sensors for data interpretation [10].

2.4 Seabed Logging

Seabed logging is an emerging technology that measures subsurface resistivity prior to drilling. The technique has been commercially available for over 5 years, and has been proven to reduce drilling risk in many offshore geologic environments. Seabed logging is defined as the use of controlled source electromagnetics (CSEM) for the purpose of finding hydrocarbons [11]. As the result of using electromagnetic for exploring oil beneath the earth was a success based on laboratory testing, electromagnetic methods are attractive for petroleum industry as complementary tools to seismic methods, or even standalone tools, for remote sensing of the subsurface.

The basis of the approach is the use of a mobile horizontal electric dipole (HED) source and an array of seafloor electric field receivers. The transmitting dipole emits a low frequency electromagnetic signal both into the overlying water column and downwards into the seabed. The array of sea floor receivers measures both the amplitude and the phase of the received signal that depend on the resistivity structure beneath the seabed. A survey consisting of many transmitter and receiver locations can be used to determine a multidimensional model of seafloor resistivity [12].

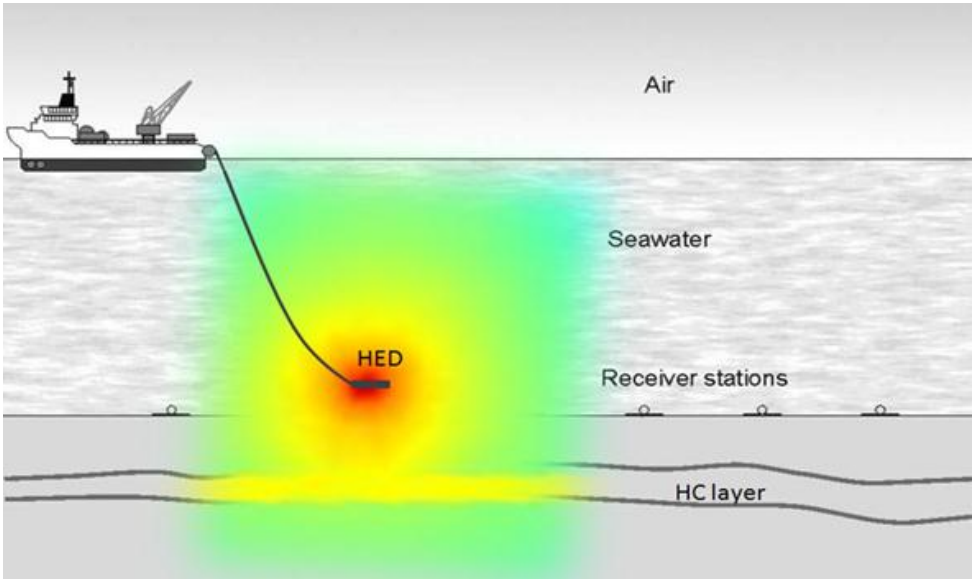

Figure 5: Seabed Logging Approach

2.5 Basic Theory in Seabed Logging

2.5.1 Skin Depth

The penetration depth is called the skin depth and surface measurement of electric and magnetic fields gives the average resistivity from the surface to a depth equivalent of the skin depth [10]. In other words, skin depth is a measure of how far the wave will penetrate into the conductivity medium. [13]. As frequency decreases, the skin depth increases. The apparent resistivity can be considered an average resistivity from the surface to the depth of the skin depth [10].

Formula for skin depth is shown as below:

$$\delta = \sqrt{\frac{2}{\mu\sigma\omega}} \approx 500m \text{ x } \sqrt{\frac{\rho}{f}}$$

Where,

δ = skin depth in meter

μ = permeability of the propagation medium

σ = conductivity of the propagation medium

ω = angular frequency of the wave

ρ = resistivity of the propagation medium

f = frequency of the wave

At a period of one second, the skin depth in seawater is about 270 meters; this means that over each 270 meters the amplitude of EM energy decays another 37 percent. In 1000 Ohm.m basalt, at the same period the skin depth is nearly 16 kilometers; so energy will propagate from the transmitter to the seafloor receivers mostly through seafloor rocks, making the method sensitive mainly to seafloor geology [14].

2.5.2 Electromagnetic (EM) Waves

In electrostatic, the electric field (E) and the electric flux density (D) are related to each other through permittivity (ε) of the region as shown in equation below [15].

$$\vec{D} = \varepsilon\vec{E}$$

Where,

D = electric flux density

ε = permittivity of the region

E = electric field

In magnetostatics, the magnetic field (B) and magnetic field intensity (H) are related to each other through permeability (μ) of the region [15]. The relation is shown as in following equation:

$$\vec{B} = \mu\vec{H}$$

Where,

B = magnetic field

μ = permeability of the region

H = magnetic field density

The source of an electromagnetic field is a distribution of electric charge and current [16]. In Maxwell's equations, it is stated that magnetic field (B) produced is proportionally related to the current and the type of the material used. The bigger the current flows inside a conductor and the higher the permeability of the material, the bigger the magnetic field is produced [17].

The relation of magnetic field, the current and the material used is shown as in equation below:

$$B = \frac{\mu I}{2\pi r}$$

Where,

B = magnetic field

μ = permeability of the material used

I = current

r = distance

There are four fundamental equations in Maxwell's equation which is shown in table below:

Table 1: Maxwell's Fundamental Equation [15]

Maxwell's equations in differential or point form	
i. $\nabla . \overrightarrow{D} = \rho_v$	Gauss's Law
ii. $\nabla \text{ X } \vec{E} = \frac{\delta \vec{B}}{\delta t}$	Conservation of Electric Field
iii. $\nabla . \vec{B} = 0$	Ampere's Circuital Law
iv. $\nabla \text{ X } \vec{H} = \vec{J} + \frac{\delta \vec{D}}{\delta t}$	Single Magnetic Pole Cannot Exist i.e Conservation of Magnetic Flux

In electromagnetic waves propagation, the magnetic field (B) and electric field (E) is perpendicular to each other with the same amplitude of reduction. Reduction of magnetic field (B) will cause same amount of reduction for electric field (E) [17].

A plane electromagnetic wave is a wave travelling from a very distant source. As shown in Figure 6, both magnetic and electric fields take place perpendicular to the *x*-axis and are therefore perpendicular to the direction of the waves. In the figure, electric field (E) is in *y*-direction while the magnetic field (B) is in *z*-direction [18].

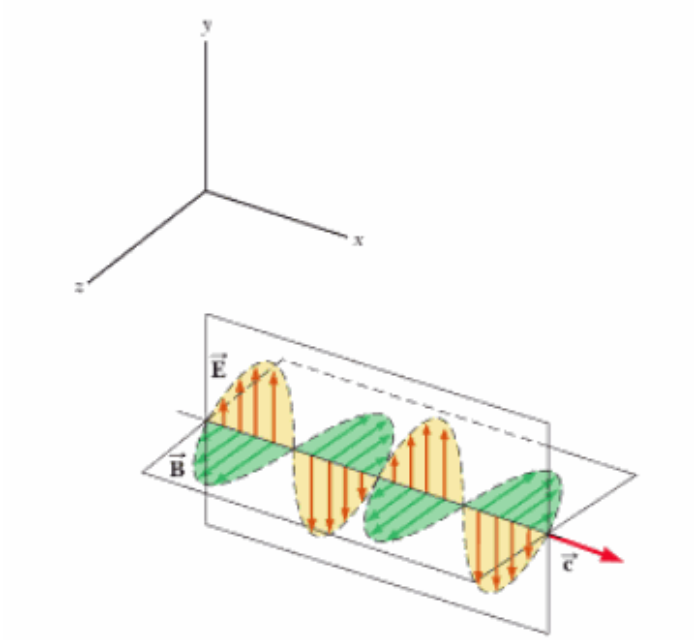

Figure 6 : Electromagnetic Waves Propagation

Electromagnetic waves travel with the speed of light. In fact, it can be shown that the speed of electromagnetic wave is related to the permeability and permittivity of the medium through which it travels and the relation is an equation followed [18]:

$$c = \frac{1}{\sqrt{\mu_o \varepsilon_o}}$$

Where,

c = speed of light

μ_o = permeability constant of the vacuum ($4\pi \times 10^{-7}$ N.s^2/C^2)

ε_o = permittivity of free space (8.854×10^{-12} C^2/N.m^2)

Because electromagnetic waves travel at the same speed as light in vacuum, scientists concluded that light is an electromagnetic wave and the relation between electromagnetic waves is:

$$\frac{E}{B} = c$$

where the ratio of electric field (E) and magnetic field (B) is equal to the speed of light [18].

2.5.3 Waves Propagation in Seabed Logging

Seabed Logging uses electromagnetic waves to distinguish the two liquids (water and hydrocarbon) based on their large differences in resistivity values. Sea water layer has a resistivity of 0.5-2 Ωm while the sediments has a resistivity of 1-2 Ωm. Hydrocarbon reservoirs are known to have resistivity value between 30-500 Ωm and it acts as the insulator as the resistivity is high compare to both sea water and the sediments. SBL uses a HED source that is towed by a vessel about 30m above an array of seafloor receivers and typically emitting frequency between 0.1 to 10Hz [19].

In designing simulation using COMSOL, there are some important characteristics need to be followed. Figure 7 shows the overburden is set as 1000m thick with resistivity of 1 Ωm and relative permittivity of 20. For hydrocarbon, the thickness is 50m with resistivity of 50 Ωm and relative permittivity of 6 [20].

In Figure 7, solid line indicates the reflected waves and the dash dot line indicated the refracted waves. Reflection is a condition when the waves, whether physical or electromagnetic, bounce from a surface back toward the source. A mirror reflects the image of the observer. Whereas the Refraction is when waves, whether physical or electromagnetic, are deflected when the waves go through a substance and generally changes the angle of its general direction [20].

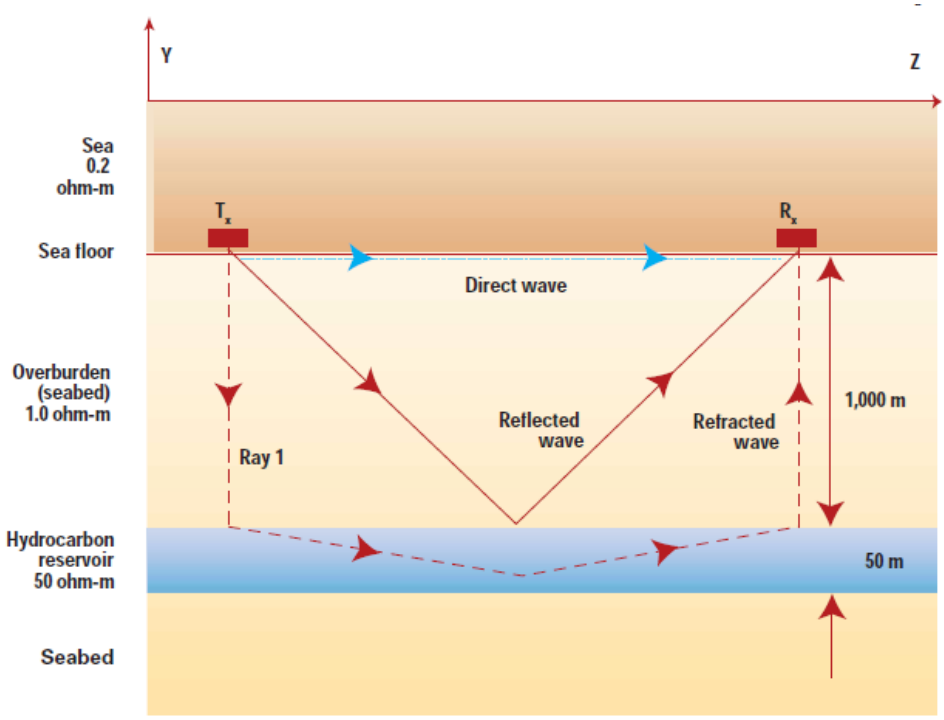

Figure 7: The Waves Propagation for Seabed Logging

2.6 Frequency Domain Method

Frequency Domain Methods are best for analyzing resonant structures and continuous wave excitation. In subsurface sensing and imaging, the most popular frequency-domain methods used are:

i. The Finite Difference Frequency Domain (FDFD)
ii. The Finite Element Method (FEM)
iii. Method of Moments (MoM)

2.6.1 The Finite Difference Frequency Domain (FDFD)

FDFD utilizes the frequency domain representation of Maxwell's equation. In practice, however, rather than Maxwell's equations, the frequency domain wave equation is more often used as it is more compact form, requires only a single field and does not require interleaving compared to Finite Difference Time Domain (FDTD) which is useful only when a single-frequency solution to a problem is sought, or when the source wave can be approximated by a single frequency. In 2D TM mode, the wave equation can be written as [21]

$$\frac{\partial^2 E_z}{\partial x^2} + \frac{\partial^2 E_z}{\partial y^2} - \gamma^2 E_z = j\omega\mu J_z$$

Where the complex propagation constant is given by:

$$\gamma^2 = j\omega\mu\sigma - \omega^2\mu\epsilon = j\omega\mu(\sigma + j\omega\epsilon)$$

2.6.2 The Finite Element Method (FEM)

FEM is also known as Finite Element Analysis (FEA). The two primary reasons for using FEM rather than FDTD for electromagnetic problems are its geometric flexibility and the ability to work in higher orders of accuracy. In finite element, one makes an approximation to the solution of the differential equation over the domain of the problem and then tailors that approximation to minimize the difference between it and the ideal, exact solution [21].

2.6.3 Methods of Moments (MoM)

MoM is based on expanding all continuous functions in terms of bases of orthogonal functions defined on each of the surfaces. These functions are usually non-overlapping functions centered at sampling points defines by a grid on the surface [22].

CHAPTER 3
METHODOLOGY

3.1 Research Methodology

In order to achieve the main objective of the project, there are 2 sub-objectives to be accomplished in the first place which are:

i. Have basic knowledge on how seabed logging works.
ii. Generating a seabed model using COMSOL

In gathering the data for seabed logging which later will be used to generate a forward mathematical model, students need to have a basic knowledge on the structure of the seabed. The properties of the hydrocarbon also need to be concerned in order to generate the seabed model. Furthermore, to have basic knowledge on how seabed logging works is important in order to interpret and analyze the data later.

After the research on the seabed structure and theoretical background of seabed completed, the next thing to learn is to generate a simulation for seabed logging as all data will be collected based on the simulation. Then, the collected data will be analyzed to generate a forward mathematical model

3.2 Procedure Identification

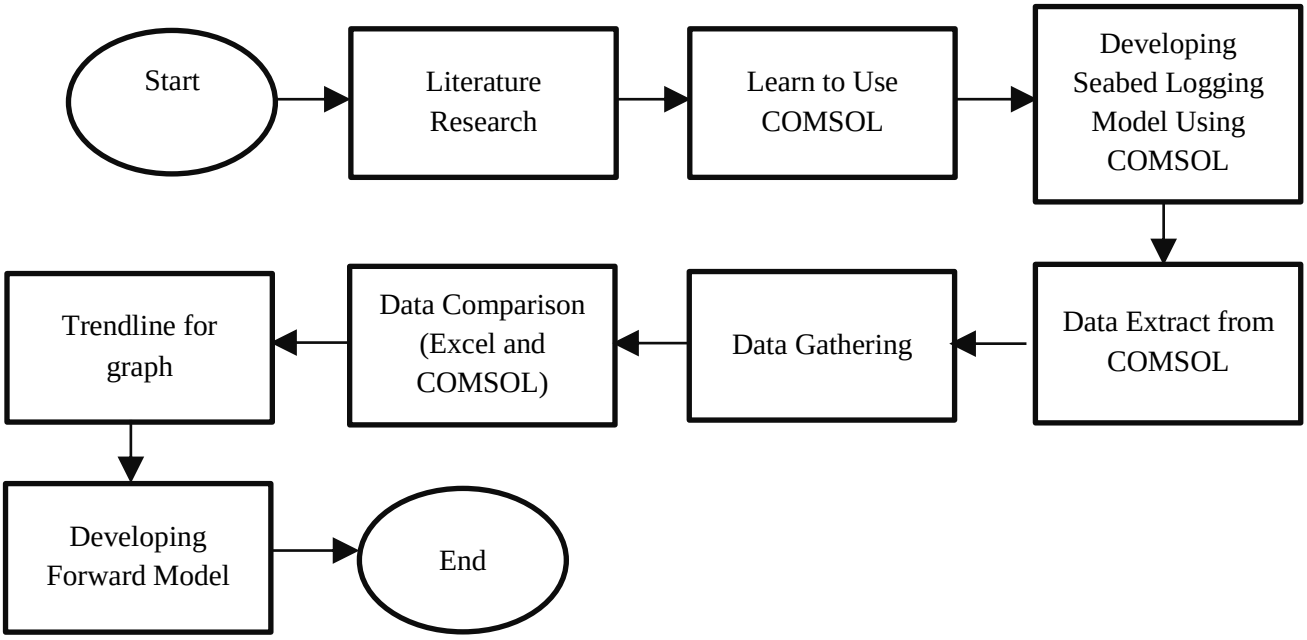

Figure 8: Flow Chart of the Project

For Final Year Project 1, the focus is more to gain knowledge on seabed logging environment. Next, author need to learn to use COMSOL software to develop the seabed model. Using COMSOL, the simulation is run and the data from COMSOL software were extracted and gathered. For Final Year Project 2, the focus was more on the analysis of the data gathered. There were some steps on the data analysis. First, using the data gathered, graphs were developed using Microsoft Excel Software. Then, the data from Excel were compared with the data from COMSOL. Next, trend line is added to the graph developed and lastly, forward mathematical models were developed.

3.3 Gantt Chart

Table 2: Gantt chart for Final Year Project 1

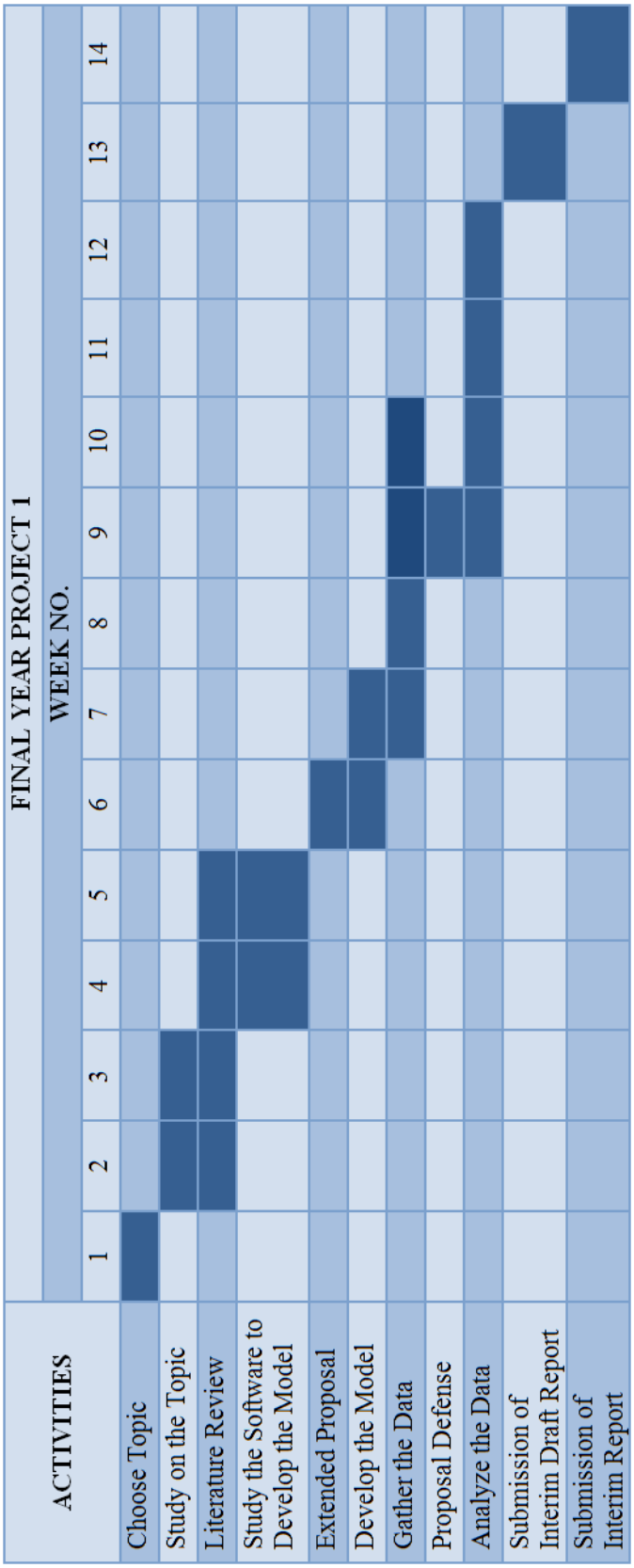

Table 3: Gantt chart for Final Year Project 2

ACTIVITIES	FINAL YEAR PROJECT 2													
	WEEK NO.													
	1	2	3	4	5	6	7	8	9	10	11	12	13	14
Data Extract from COMSOL														
Data Gathering														
Data Comparison														
Data Analysis (Graph Trendline)														
Progress Report														
Developing Forward Mathematical Models														
Technical Paper														
Draft Report														
Final Report														

3.4 Tool Required

In this project, software COMSOL Multiphysic is required to generate a seabed model simulation in order to collect the data which will later be used to generate the forward mathematical model. COMSOL is a powerful interactive environment for modeling and solving all kinds of scientific and engineering problems based on partial differential equations (PDEs). With this software, it will be easy for the author to extend conventional models of one type of physics into mutiphysics models that solve coupled physic phenomena. COMSOL can also be used to compile sets of PDEs which represent the entire model. This software also is a standalone product with a graphical user interface.

Figure 9: COMSOL MultiPhysic Software

CHAPTER 4
RESULT AND DISCUSSION

4.1 COMSOL Multiphysics Simulation

Some 3D models for Seabed Logging have been developed using COMSOL and the models were modified to observe the difference on the result by changing the following parameters:

1) Depth of the hydrocarbon
2) Frequency of the Transmitter

There are 4 main layers for the seabed model and each layer is fixed with the following properties:

Table 4: Properties of Layer for Seabed Model in Meter

	Air	**Sea**	**Sediment**	**Hydrocarbon**
X (Length)	10 000	10 000	10 000	10 000
Y (Width)	5 000	5 000	5 000	5 000
Z (Height)	500	2 000	4 000	100

Sediment contains 2 parts which is overburden and underburden. Overburden is sediment located above the hydrocarbon layer while underburden is sediment located below the hydrocarbon layer.

For this project, initial location of the hydrocarbon is 1000m below the seabed (1000m overburden layer) and will increase with 250m increment until 3000m. For the transmitter, there are four frequencies used which are 0.5Hz, 0.25Hz, 0.125Hz and 0.0625Hz. The transmitter used is 270m long and is located 30m above the seabed layer while the receiver is represented by a straight line parallel to the transmitter and placed at the seabed. Figure 10 shows the rough model for 3D seabed model.

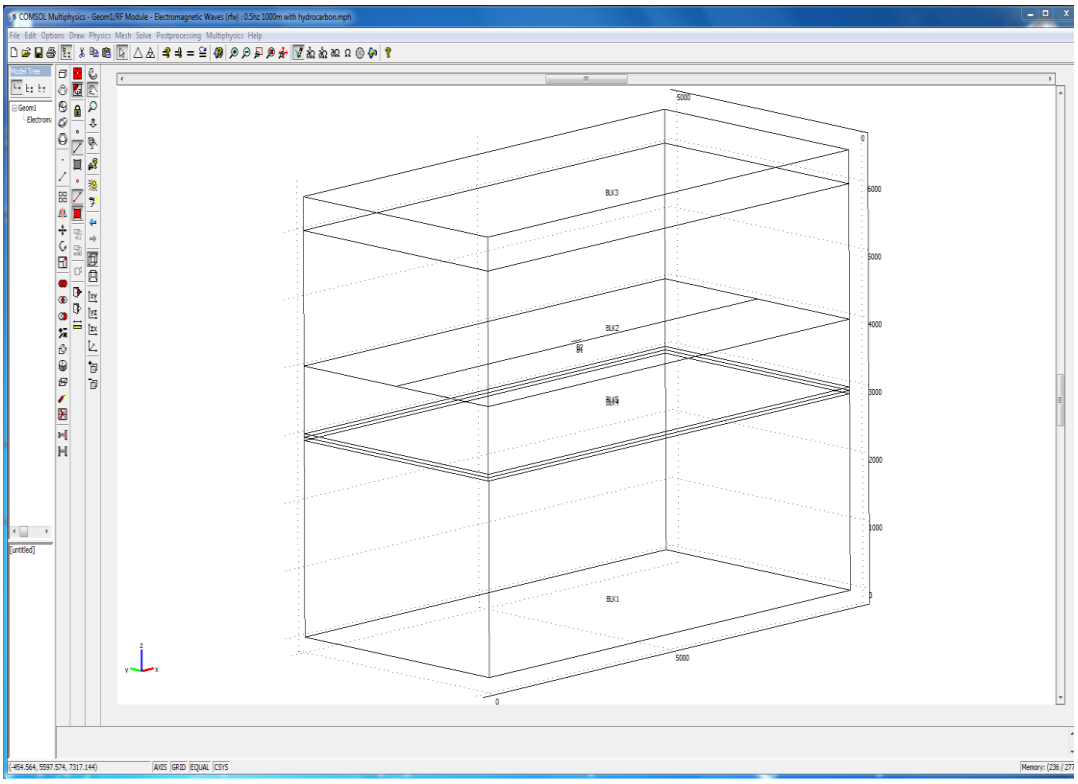

Figure 10: Layers for 3D Model of Seabed Logging

The E-field generated from model with hydrocarbon was compared to the model without the hydrocarbon in SBL environment. Table 2 and Table 3 show the parameter setting for model with and without hydrocarbon.

Table 5: Parameter Setting for SBL with hydrocarbon

Setting	Sea water	Hydrocarbon	Air	Sediment
Relative Permittivity	80	4	1	30
Electric Conductivity	3	0.01	1e-12	1.5

Table 6: Parameter Setting for SBL without hydrocarbon

Setting	Sea water	Hydrocarbon	Air	Sediment
Relative Permittivity	80	30	1	30
Electric Conductivity	3	1.5	1e-12	1.5

4.1.1 Result for Varying the Depth of the Hydrocarbon

After the model of the seabed model was constructed and all the parameters were assigned, meshing had been done to the geometry to get the number of mesh element. Figure 11 shows the SBL model with hydrocarbon and area that has large number of mesh element is where the hydrocarbon was located. (Location of the hydrocarbon is 1000m below seabed)

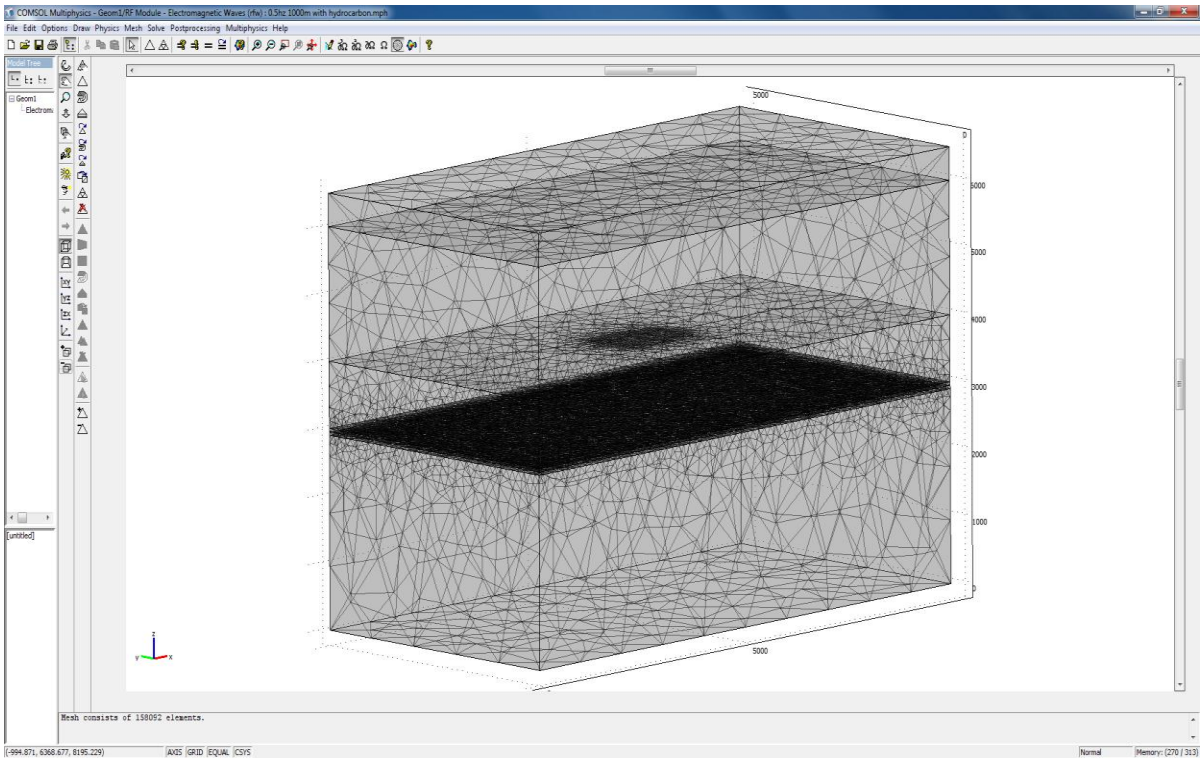

Figure 11: Mesh Geometry of the SBL Environment

Next step is to solve the model. Area that has red color has highest total energy density. From Figure 12, the area with red color is showed by the transmitter because the transmitter is the central point where the EM waves will transmit through the seabed. As the frequency goes further, energy will reduce and after a certain point, it will completely dissolve.

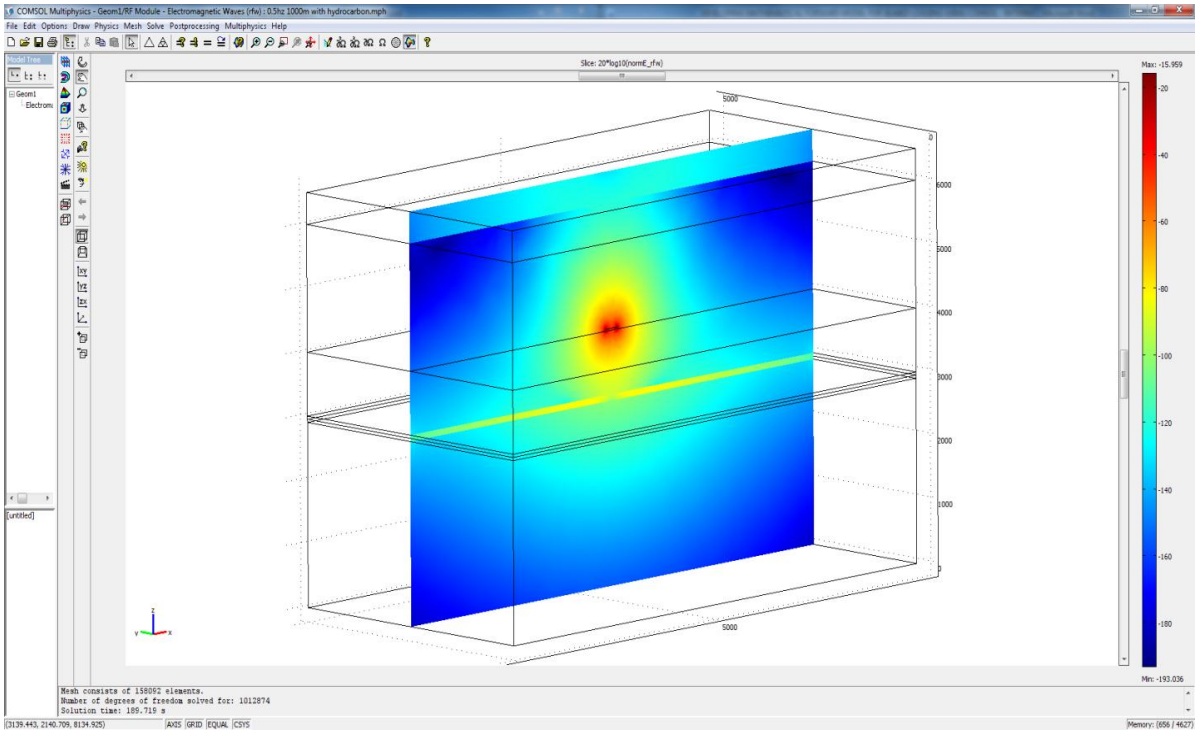

Figure 12: Energy Density at Linear Scale

Ranges for 3D Seabed models are 1000m, 1250m, 1500m, 1750m, 2000m, 2250m, 2500m, 2750m and 3000m with frequency 0.5Hz. The simulation is then repeated using different frequencies which are 0.25Hz, 0.125Hz and 0.0625Hz and the result is compared in the next section.

- Hydrocarbon layer is at minimum depth, z= 1000m

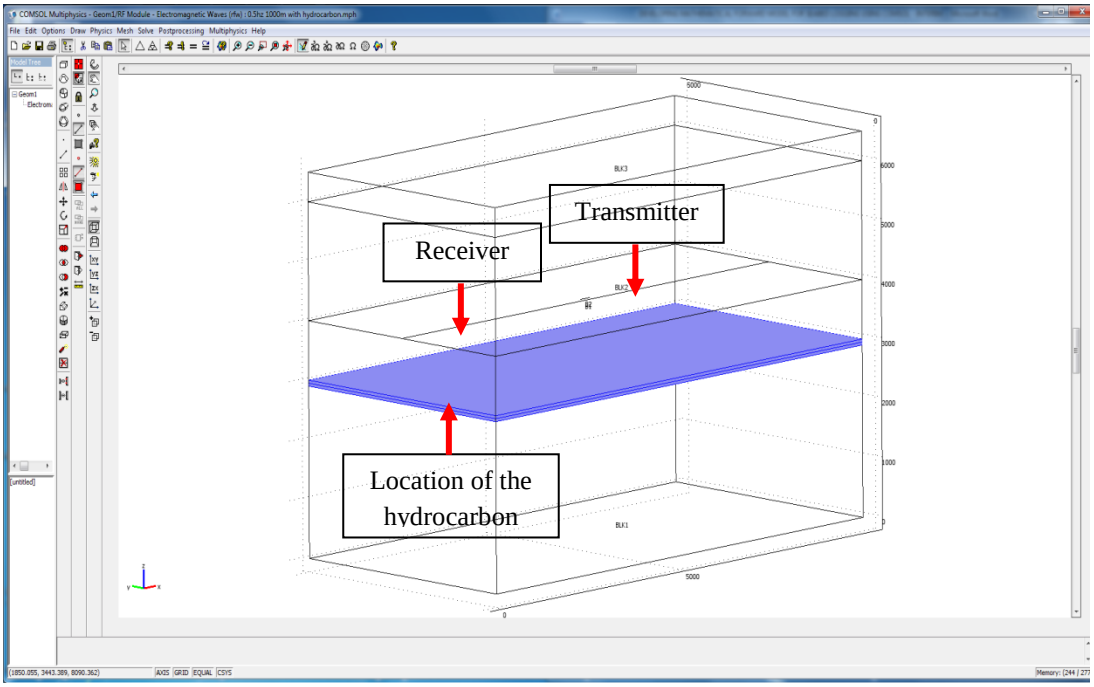

Figure 13: Hydrocarbon Location at Depth 1000m below the Sea Floor

- Hydrocarbon layer is at maximum depth, z= 3000m

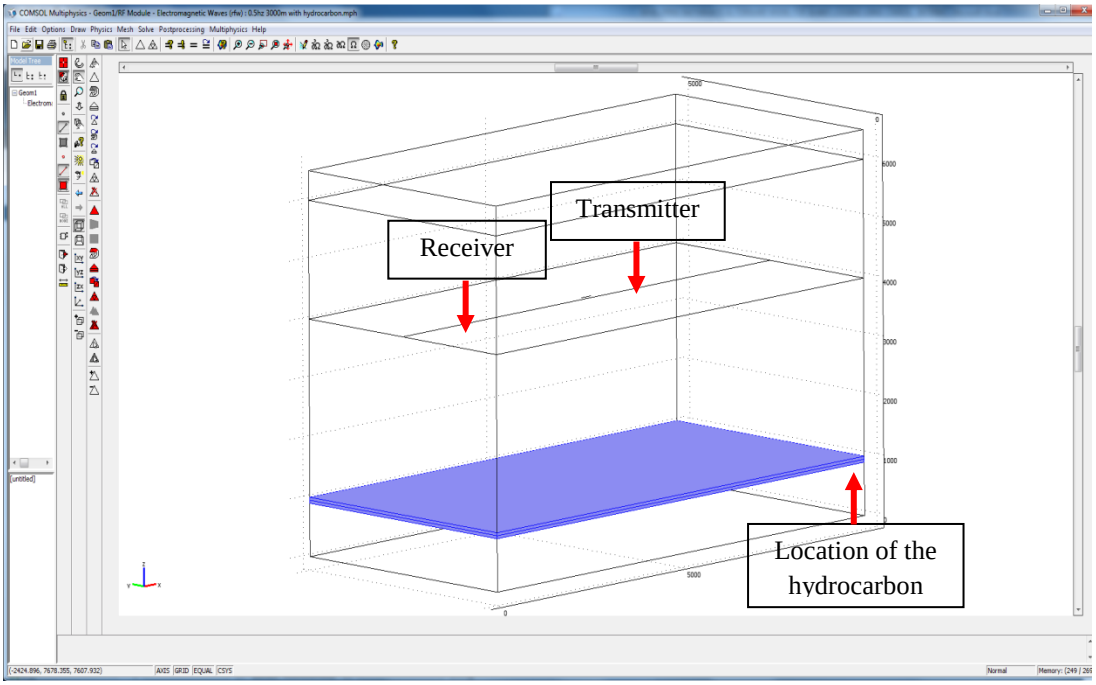

Figure 14: Hydrocarbon Location at Depth 3000m below the Sea Floor

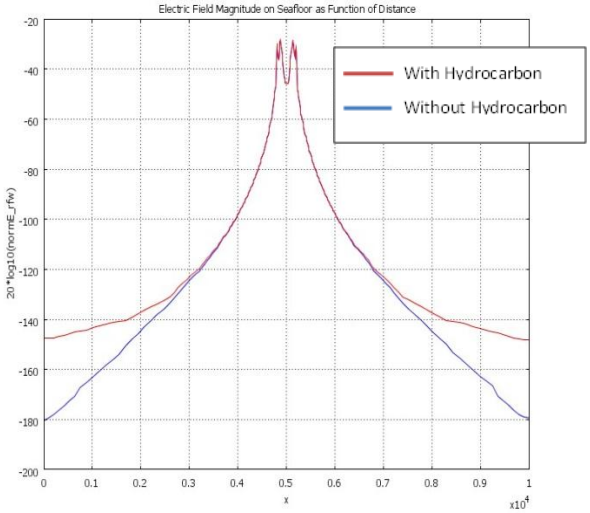

Figure 15: Magnitude of E-Field at Depth 1000m with Frequency 0.5Hz

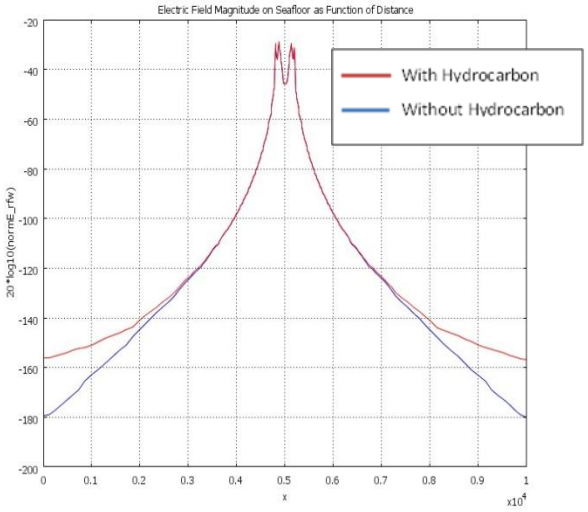

Figure 16: Magnitude of E-Field at Depth 1250m with Frequency 0.5Hz

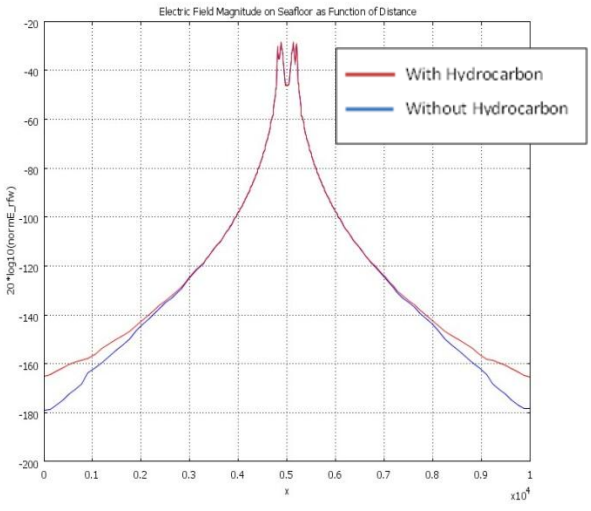

Figure 17: Magnitude of E-Field at Depth 1500m with Frequency 0.5Hz

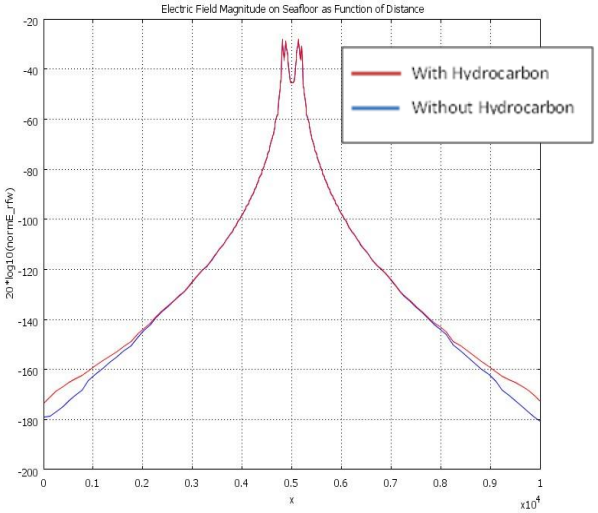

Figure 18: Magnitude of E-Field at Depth 1750m with Frequency 0.5Hz

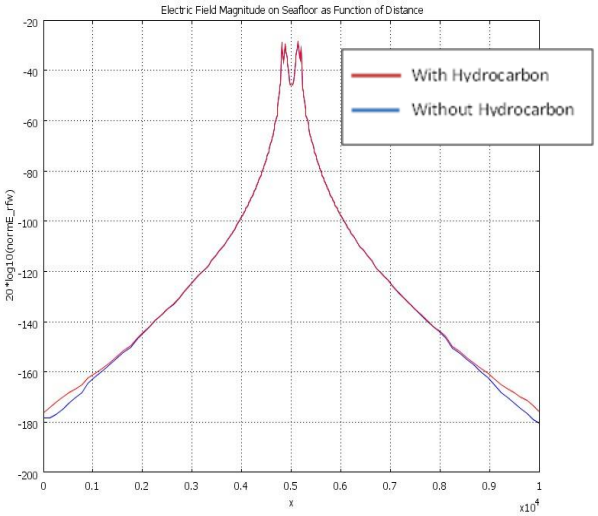

Figure 19: Magnitude of E-Field at Depth 2000m with Frequency 0.5Hz

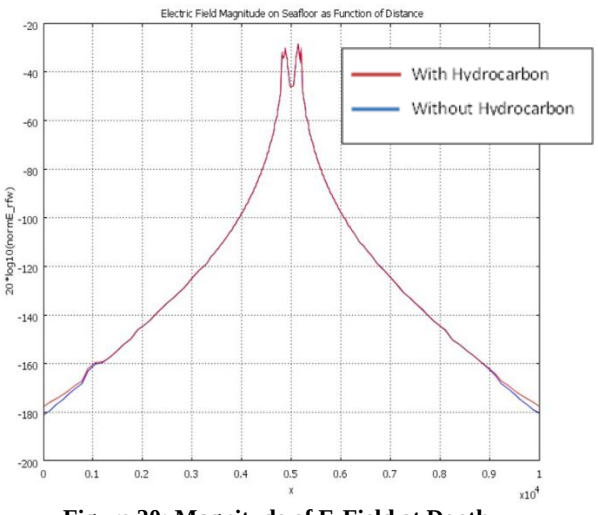

Figure 20: Magnitude of E-Field at Depth 2250m with Frequency 0.5Hz

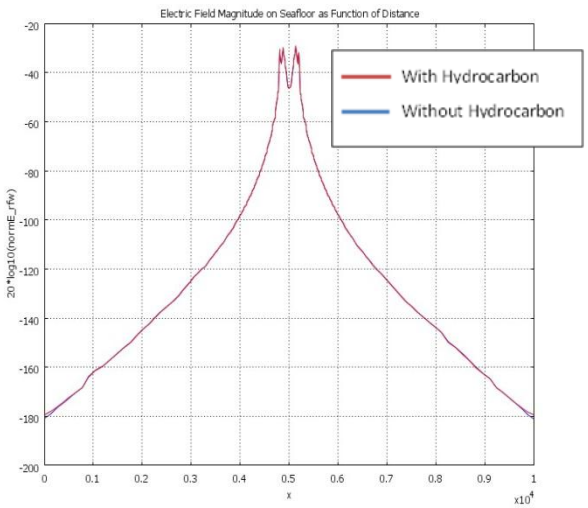

Figure 21: Magnitude of E-Field at Depth 2500m with Frequency 0.5Hz

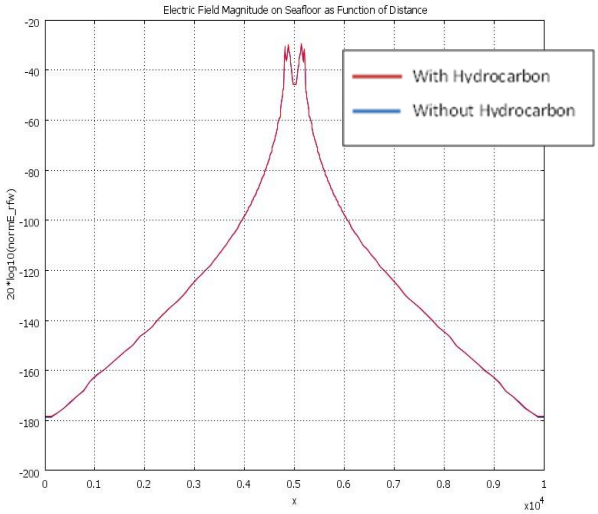

Figure 22: Magnitude of E-Field at Depth 2750m with Frequency 0.5Hz

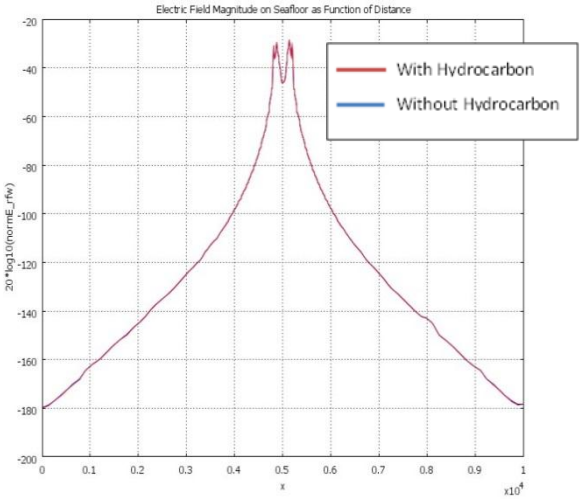

Figure 23: Magnitude of E-Field at Depth 3000m with Frequency 0.5Hz

DISCUSSION

Figures above show the magnitude of received electric field (E-Field) at the receivers from model with and without hydrocarbon at frequency 0.5Hz. Magnitude of E-Field is reducing as the depth of the hydrocarbon is getting deeper. At depth 2500m, the magnitude of E-Field with and without hydrocarbon is almost equal with small gap at point 0m and 10km but at depth 2750m, the gap between model with and without hydrocarbon is zero and as a conclusion, limit for frequency 0.5Hz is at depth 2750m.

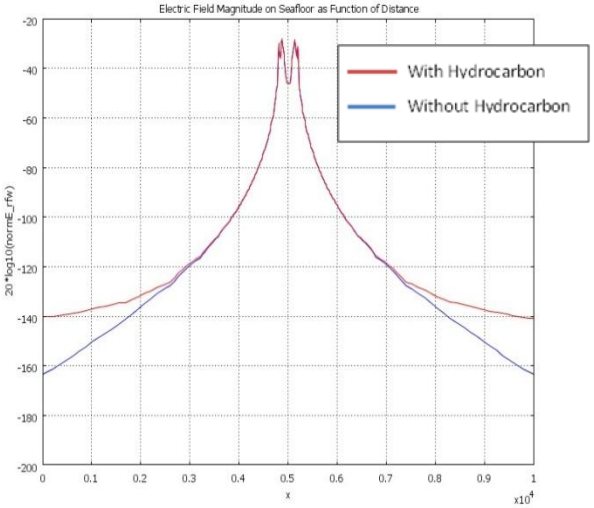

Figure 24: Magnitude of E-Field at Depth 1000m with Frequency 0.25Hz

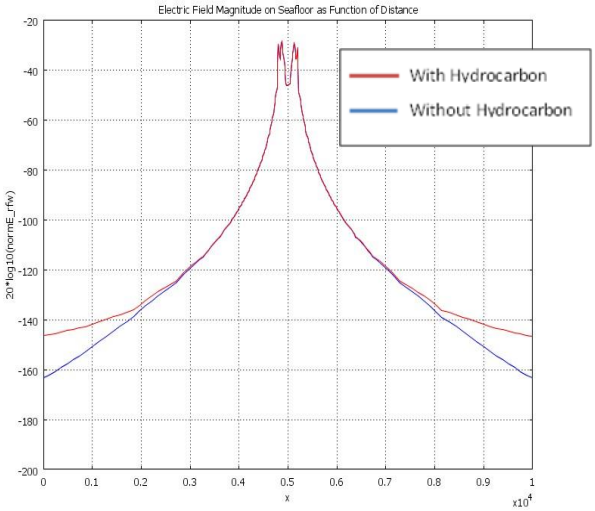

Figure 25: Magnitude of E-Field at Depth 1250m with Frequency 0.25Hz

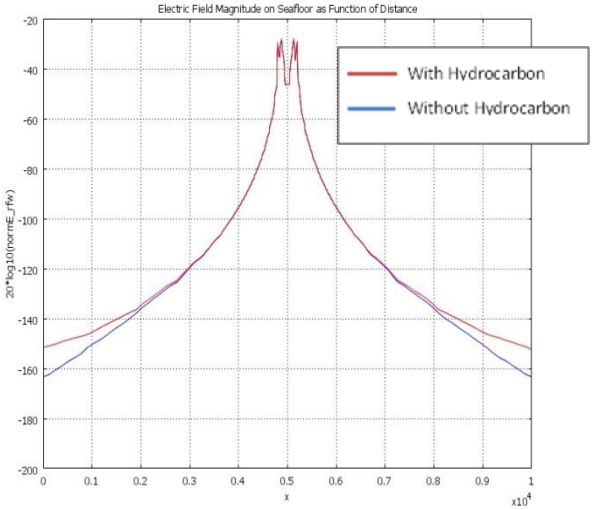

Figure 26: Magnitude of E-Field at Depth 1500m with Frequency 0.25Hz

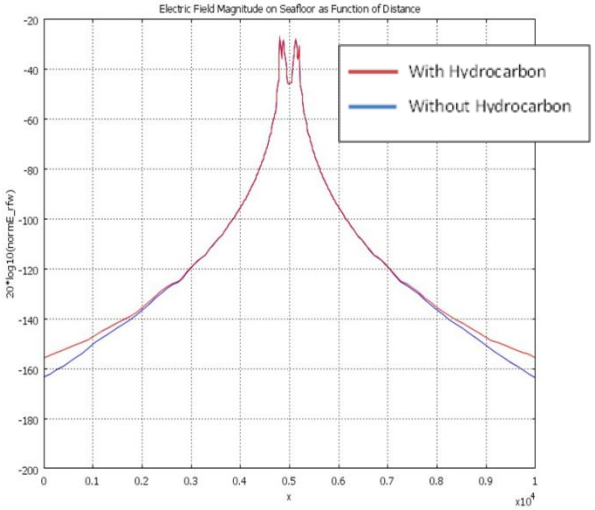

Figure 27: Magnitude of E-Field at Depth 1750m with Frequency 0.25Hz

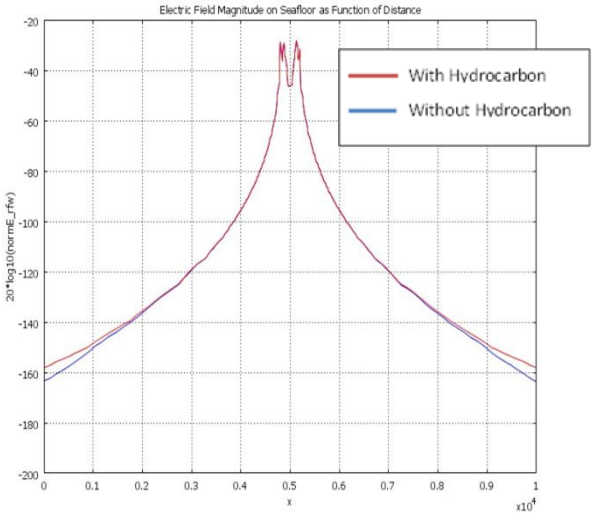

Figure 28: Magnitude of E-Field at Depth 2000m with Frequency 0.25Hz

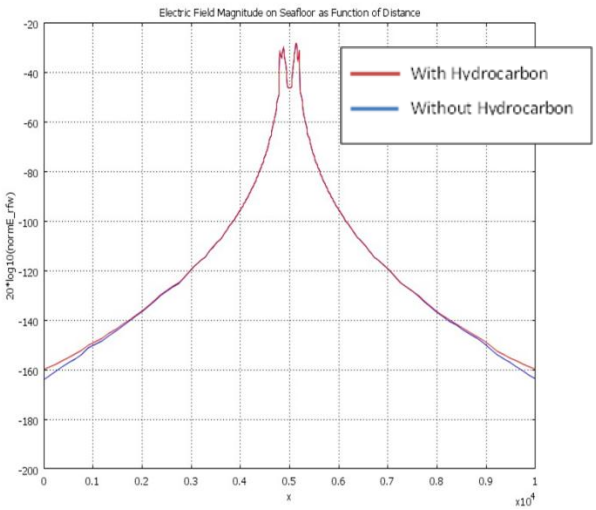

Figure 29: Magnitude of E-Field at Depth 2250m with Frequency 0.25Hz

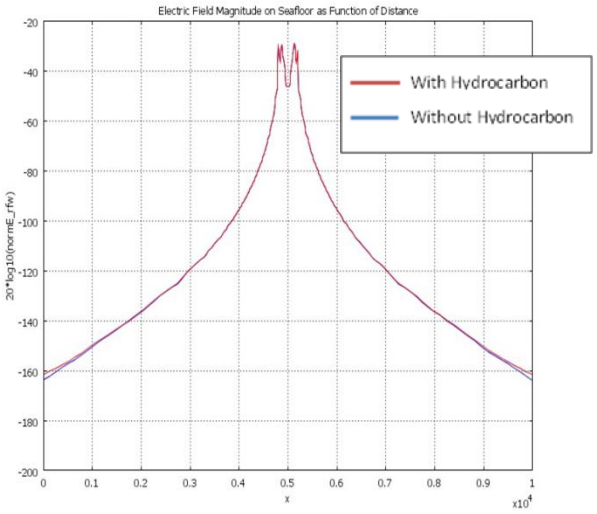

Figure 30: Magnitude of E-Field at Depth 2500m with Frequency 0.25Hz

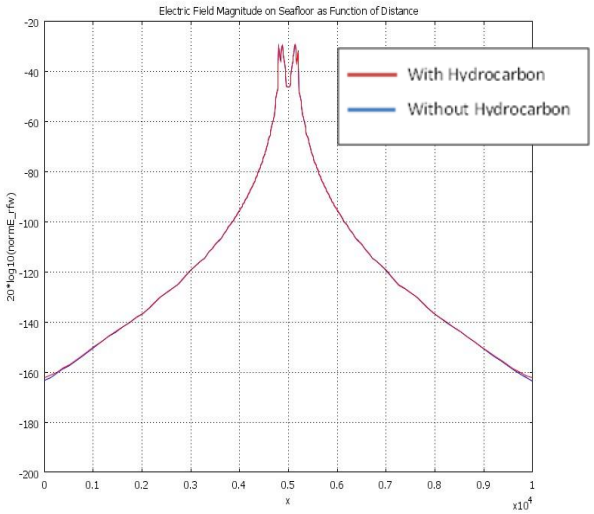

Figure 31: Magnitude of E-Field at Depth 2750m with Frequency 0.25Hz

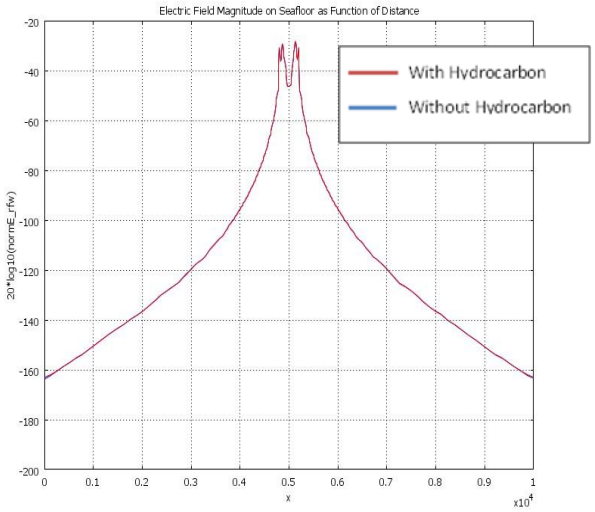

Figure 32: Magnitude of E-Field at Depth 3000m with Frequency 0.25Hz

DISCUSSION

Figures above show the magnitude of received electric field (E-Field) at the receivers from model with and without hydrocarbon at frequency 0.25Hz. Magnitude of E-Field is reducing as the depth of the hydrocarbon is getting deeper. At depth 2750m, the magnitude of E-Field with and without hydrocarbon is almost equal and at depth 3000m, the difference of E-Field magnitude between with and without hydrocarbon models are completely zero.

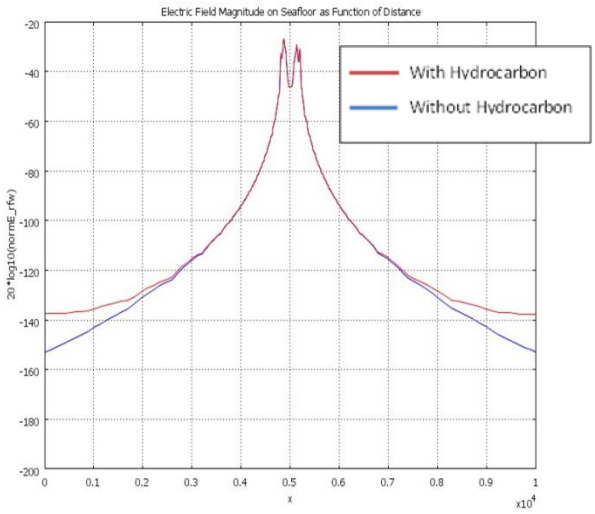

Figure 33: Magnitude of E-Field at Depth 1000m with Frequency 0.125Hz

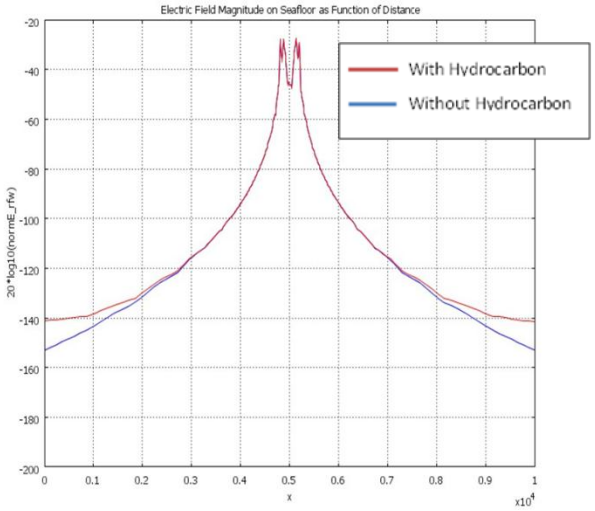

Figure 34 Magnitude of E-Field at Depth 1250m with Frequency 0.125Hz

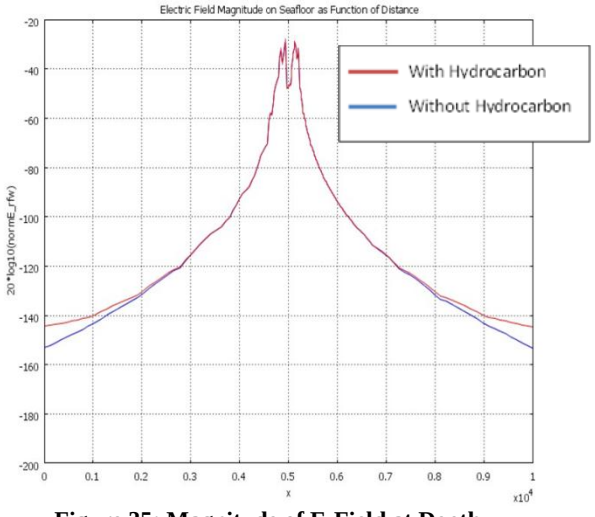

Figure 35: Magnitude of E-Field at Depth 1500m with Frequency 0.125Hz

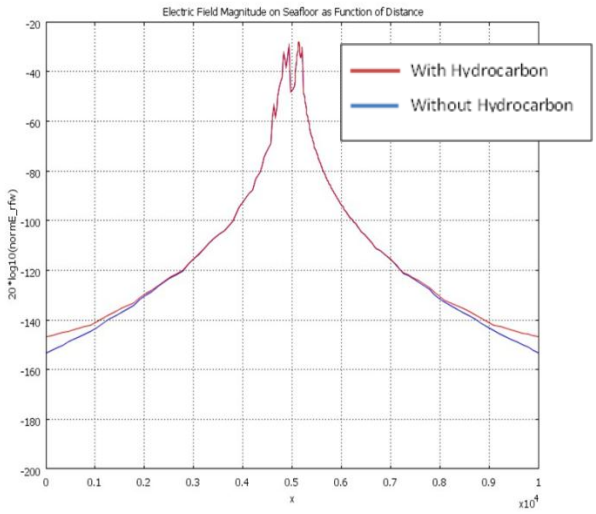

Figure 36: Magnitude of E-Field at Depth 1750m with Frequency 0.125Hz

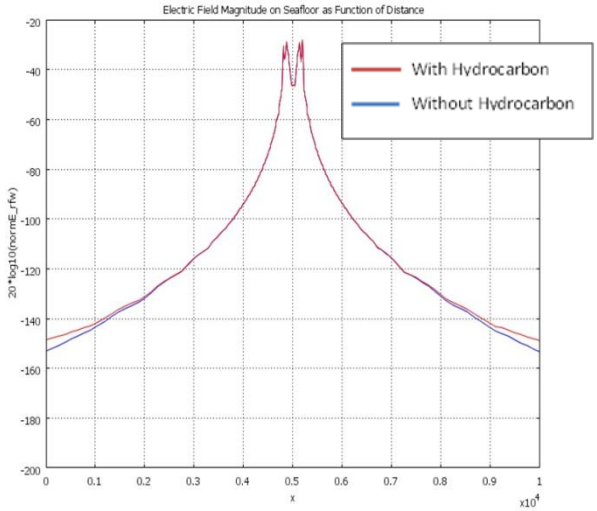

Figure 37: Magnitude of E-Field at Depth 2000m with Frequency 0.125Hz

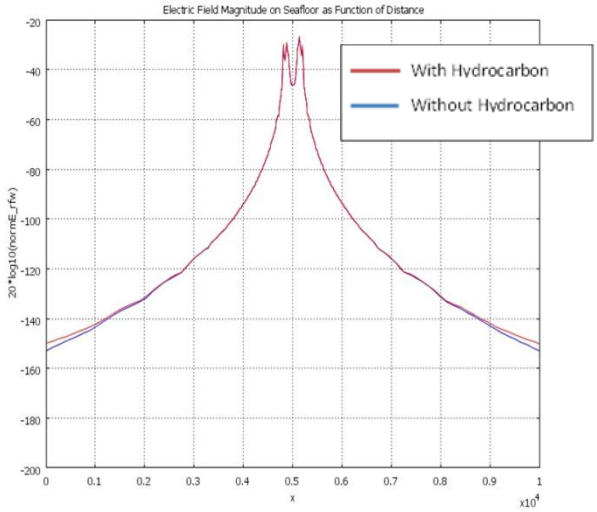

Figure 38: Magnitude of E-Field at Depth 2250m with Frequency 0.125Hz

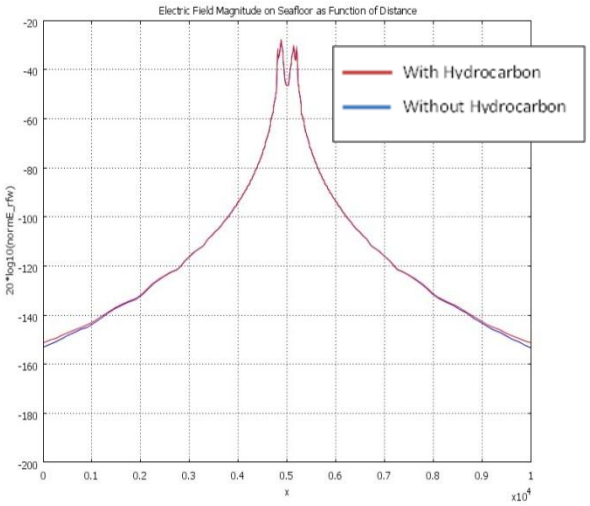

Figure 39: Magnitude of E-Field at Depth 2500m with Frequency 0.125Hz

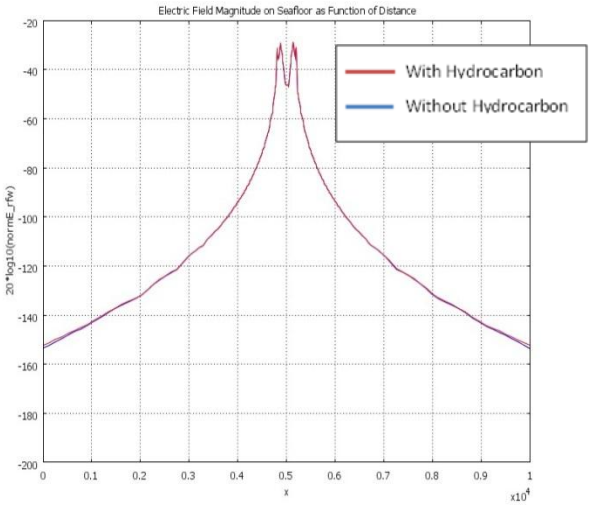

Figure 41: Magnitude of E-Field at Depth 2750m with Frequency 0.125Hz

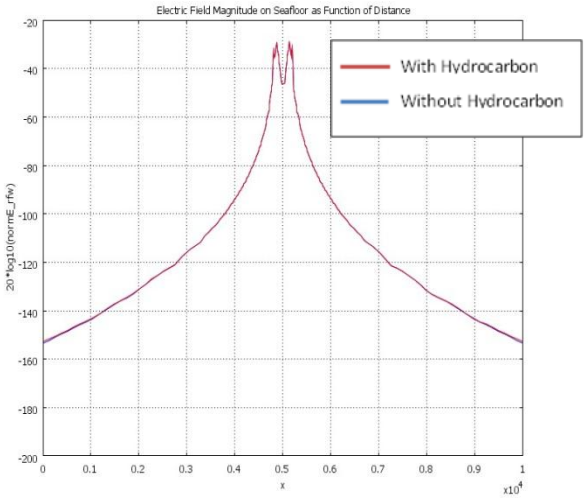

Figure 40: Magnitude of E-Field at Depth 3000m with Frequency 0.125Hz

DISCUSSION

Figures above show the magnitude of received electric field (E-Field) at the receivers from model with and without hydrocarbon at frequency 0.125Hz. Magnitude of E-Field is reducing as the depth of the hydrocarbon is getting deeper. At depth 3000m, the magnitude of E-Field with and without hydrocarbon is almost equal with a really small gap at point 0m and 10km. It shows that frequency 0.125Hz can still be used to detect the present of hydrocarbon at depth more than 3000m.

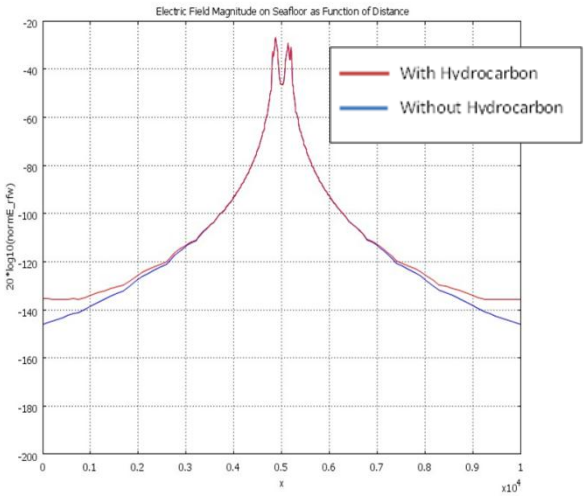

Figure 42: Magnitude of E-Field at Depth 1000m with Frequency 0.0625Hz

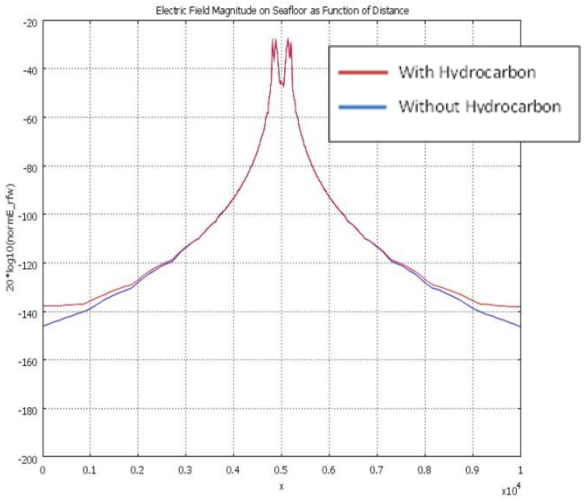

Figure 43: Magnitude of E-Field at Depth 1250m with Frequency 0.0625Hz

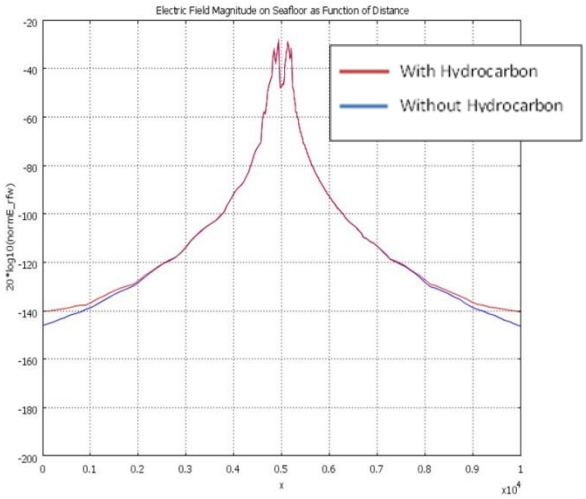

Figure 44: Magnitude of E-Field at Depth 1500m with Frequency 0.0625Hz

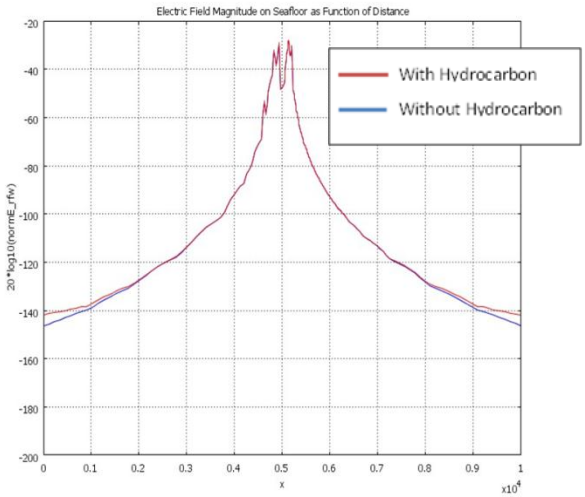

Figure 45: Magnitude of E-Field at Depth 1750m with Frequency 0.0625Hz

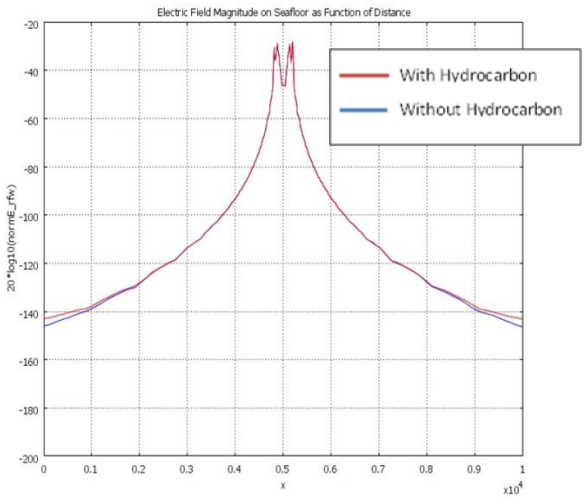

Figure 46: Magnitude of E-Field at Depth 2000m with Frequency 0.0625Hz

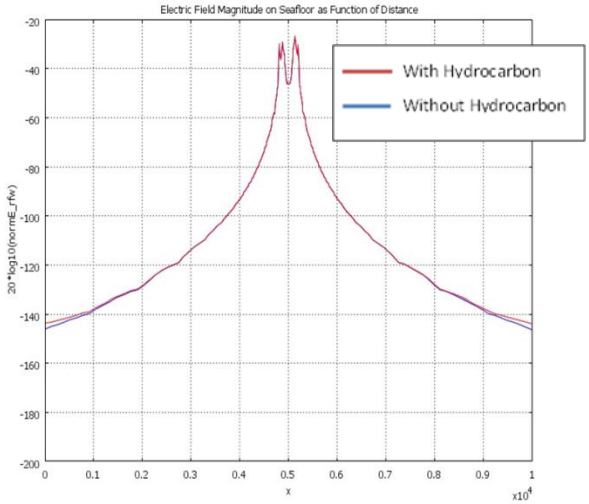

Figure 47: Magnitude of E-Field at Depth 2250m with Frequency 0.0625Hz

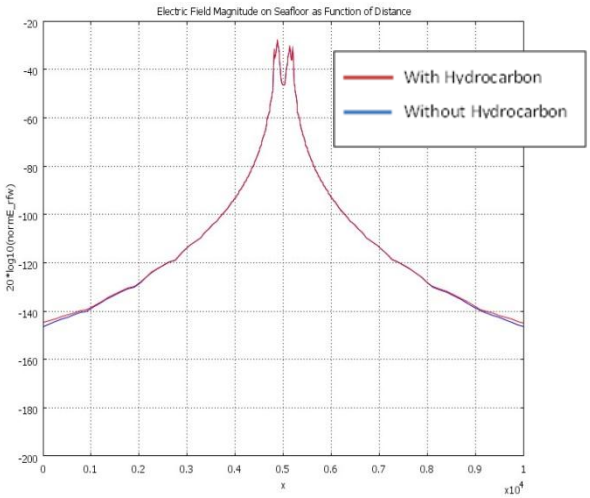

Figure 49: Magnitude of E-Field at Depth 2500m with Frequency 0.0625Hz

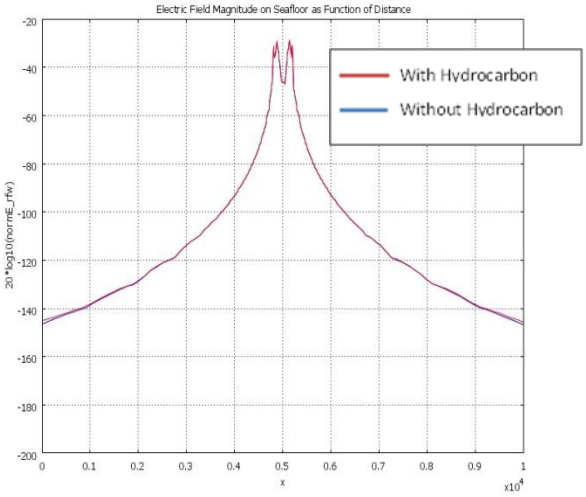

Figure 48: Magnitude of E-Field at Depth 2750m with Frequency 0.0625Hz

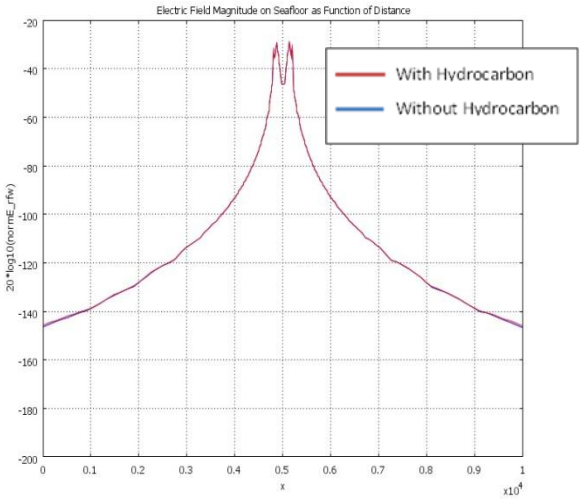

Figure 50: Magnitude of E-Field at Depth 3000m with Frequency 0.0625Hz

DISCUSSION

Figures above show the magnitude of received electric field (E-Field) at the receivers from model with and without hydrocarbon at frequency 0.0625Hz. Magnitude of E-Field is reducing as the depth of the hydrocarbon is getting deeper. At depth 3000m, the magnitude of E-Field with and without hydrocarbon is almost equal with a really small gap at point 0m and 10km. It shows that frequency 0.0625Hz can still be used to detect the present of hydrocarbon at depth more than 3000m.

4.1.2 Result with Varying Frequency of the Transmitter

Second part of the project was comparing the magnitude of the hydrocarbon by varying the frequency of the transmitter. At each depth, four different frequencies had been run and the magnitude of the E-Field was recorded in results section.

RESULT AT DEPTH 1000m:

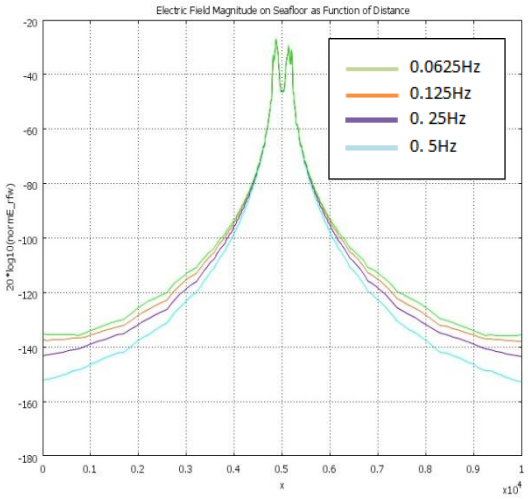

Figure 51: Magnitude of E-Field at Depth 1000m for Frequency 0.5Hz, 0.25Hz, 0.125Hz and 0.0625Hz

RESULT AT DEPTH 1500m:

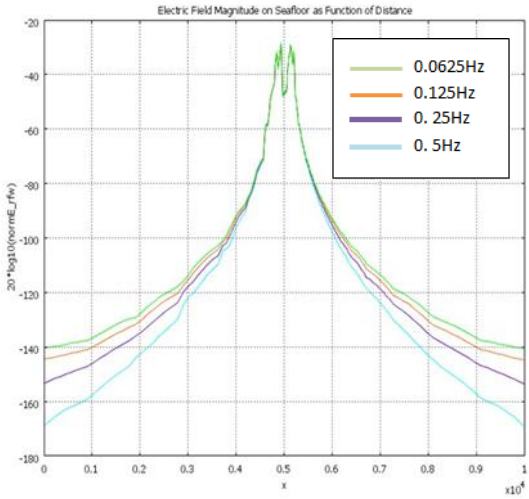

Figure 53: Magnitude of E-Field at Depth 1500m for Frequency 0.5Hz, 0.25Hz, 0.125Hz and 0.0625Hz

RESULT AT DEPTH 1250m:

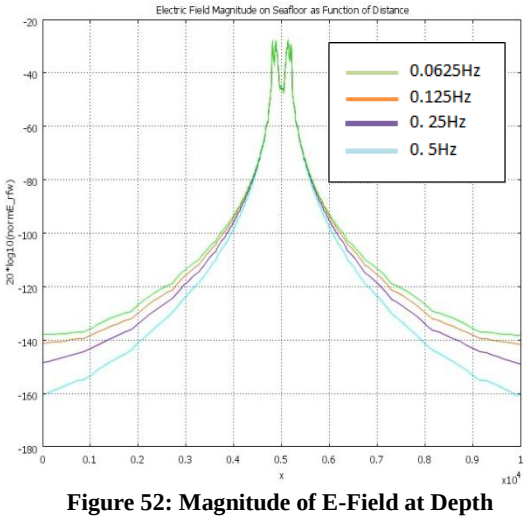

Figure 52: Magnitude of E-Field at Depth 1250m for Frequency 0.5Hz, 0.25Hz, 0.125Hz and 0.0625Hz

RESULT AT DEPTH 1750m:

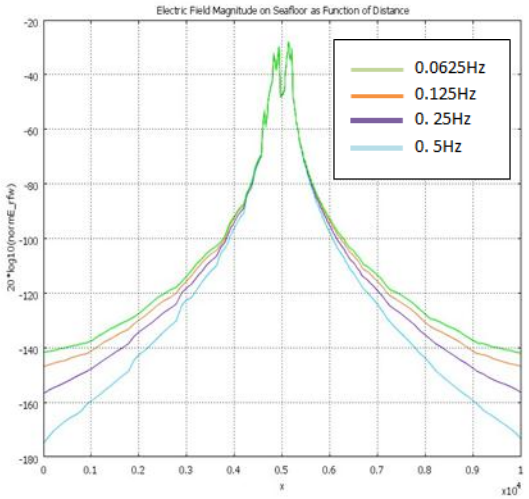

Figure 54: Magnitude of E-Field at Depth 1750m for Frequency 0.5Hz, 0.25Hz, 0.125Hz and 0.0625Hz

RESULT AT DEPTH 2000m:

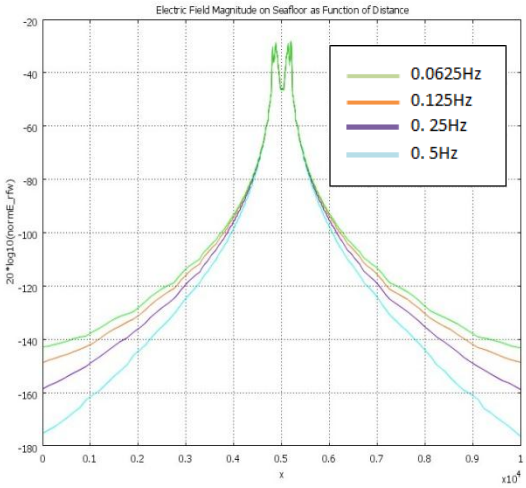

Figure 55: Magnitude of E-Field at Depth 2000m for Frequency 0.5Hz, 0.25Hz, 0.125Hz and 0.0625Hz

RESULT AT DEPTH 2250m:

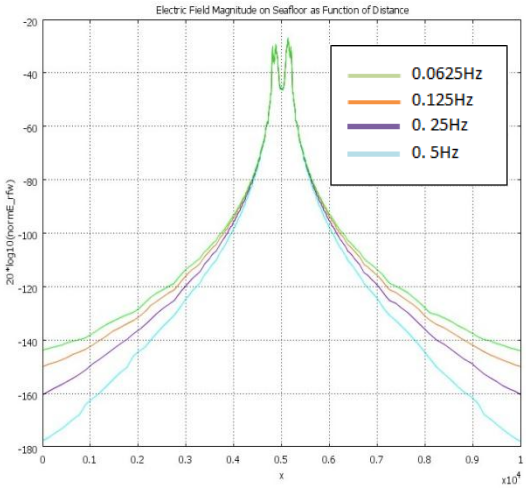

Figure 56: Magnitude of E-Field at Depth 2250m for Frequency 0.5Hz, 0.25Hz, 0.125Hz and 0.0625Hz

RESULT AT DEPTH 2500m:

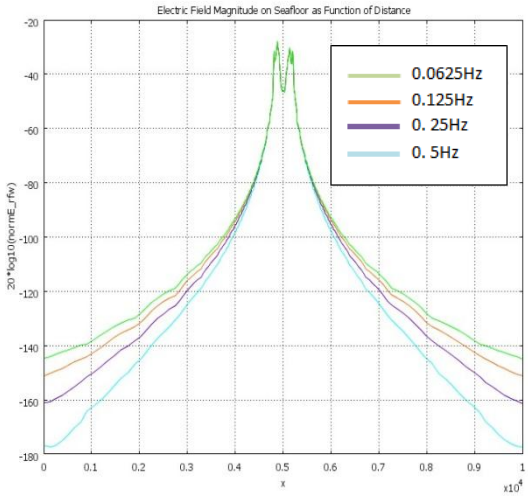

Figure 57: Magnitude of E-Field at Depth 2500m for Frequency 0.5Hz, 0.25Hz, 0.125Hz and 0.0625Hz

RESULT AT DEPTH 2750m:

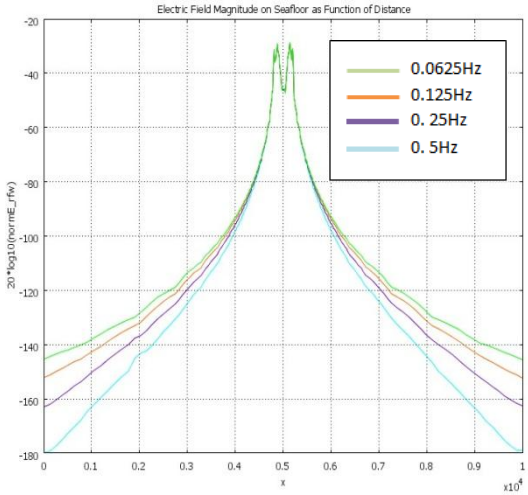

Figure 58: Magnitude of E-Field at Depth 2750m for Frequency 0.5Hz, 0.25Hz, 0.125Hz and 0.0625Hz

RESULT AT DEPTH 3000m:

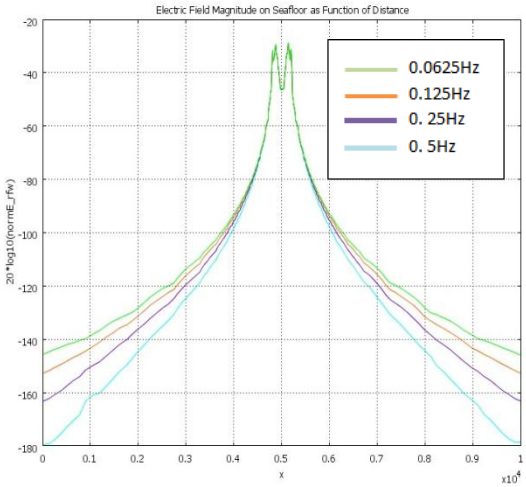

Figure 59: Magnitude of E-Field at Depth 3000m for Frequency 0.5Hz, 0.25Hz, 0.125Hz and 0.0625Hz

DISCUSSION

As the depth going deeper, the magnitude of E-Field is getting smaller for all frequencies. Model with frequency 0.0625Hz has the highest magnitude followed by 0.125Hz, 0.25Hz and 0.5Hz of frequency. Therefore, lower frequency has bigger wavelength and higher wavelength lead to higher magnitude of E-Field.

4.2 RESULT FOR SEABED LOGGING (SBL) USING EXCEL

Focus on this part was to extract the data from COMSOL and using the data, graph was developed and compared with the graph from COMSOL. Below were the graphs from the data. This step is important to ensure that all data extract from COMSOL is correct and can be used to determine the type of mathematical model for SBL. Using the data, the graph was developed varied on the frequencies at same depth.

RESULT AT DEPTH 1000m:

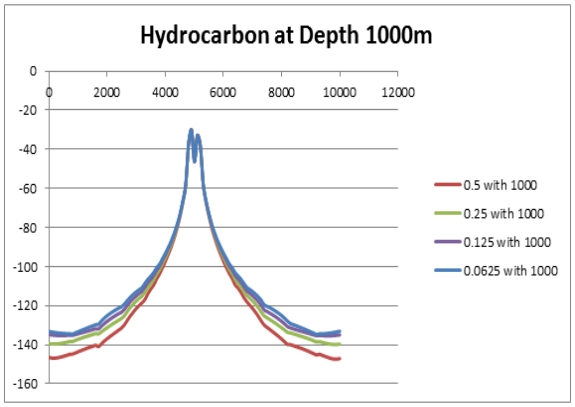

Figure 60: Magnitude of E-Field at Depth 1000m for Frequency 0.5Hz, 0.25Hz, 0.125Hz and 0.0625Hz (Excel)

RESULT AT DEPTH 1750m:

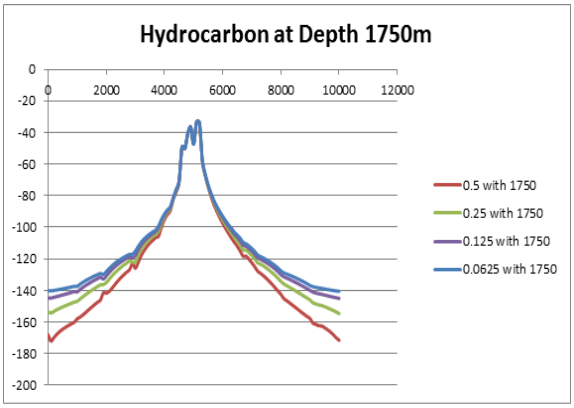

Figure 63: Magnitude of E-Field at Depth 1750m for Frequency 0.5Hz, 0.25Hz, 0.125Hz and 0.0625Hz (Excel)

RESULT AT DEPTH 1250m:

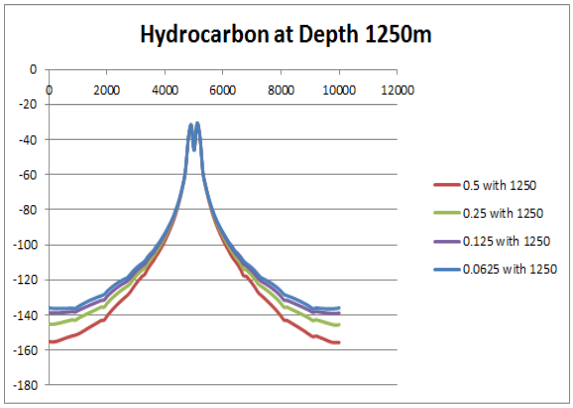

Figure 61: Magnitude of E-Field at Depth 1250m for Frequency 0.5Hz, 0.25Hz, 0.125Hz and 0.0625Hz (Excel)

RESULT AT DEPTH 2000m:

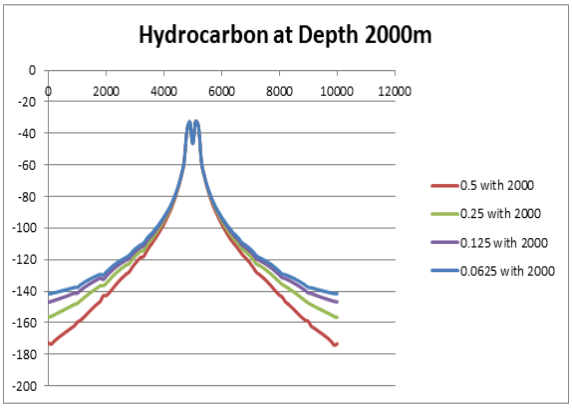

Figure 64: Magnitude of E-Field at Depth 2000m for Frequency 0.5Hz, 0.25Hz, 0.125Hz and 0.0625Hz (Excel)

RESULT AT DEPTH 1500m:

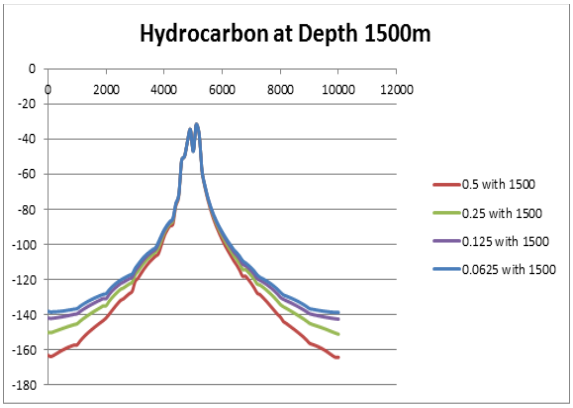

Figure 62: Magnitude of E-Field at Depth 1500m for Frequency 0.5Hz, 0.25Hz, 0.125Hz and 0.0625Hz (Excel)

RESULT AT DEPTH 2250m:

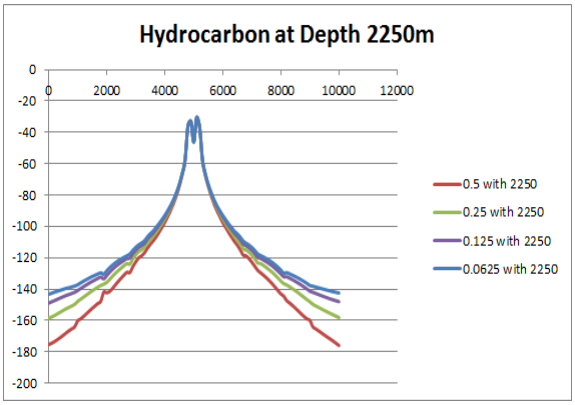

Figure 65: Magnitude of E-Field at Depth 2250m for Frequency 0.5Hz, 0.25Hz, 0.125Hz and 0.0625Hz (Excel)

RESULT AT DEPTH 2500m:

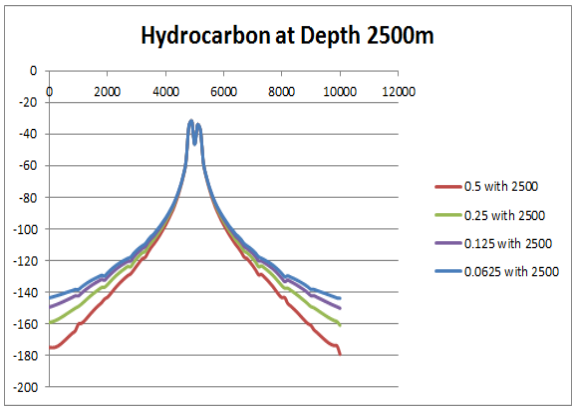

Figure 66: Magnitude of E-Field at Depth 2500m for Frequency 0.5Hz, 0.25Hz, 0.125Hz and 0.0625Hz (Excel)

RESULT AT DEPTH 2750m:

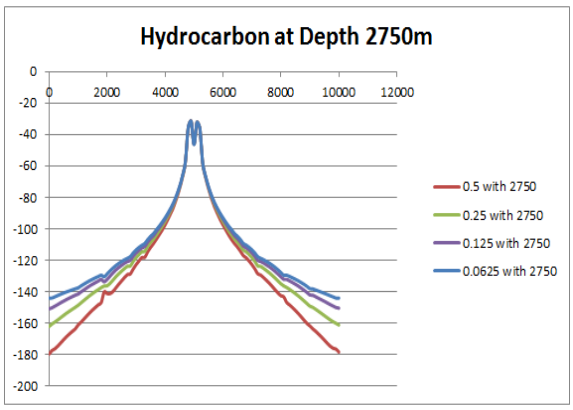

Figure 67: Magnitude of E-Field at Depth 2750m for Frequency 0.5Hz, 0.25Hz, 0.125Hz and 0.0625Hz (Excel)

RESULT AT DEPTH 3000m:

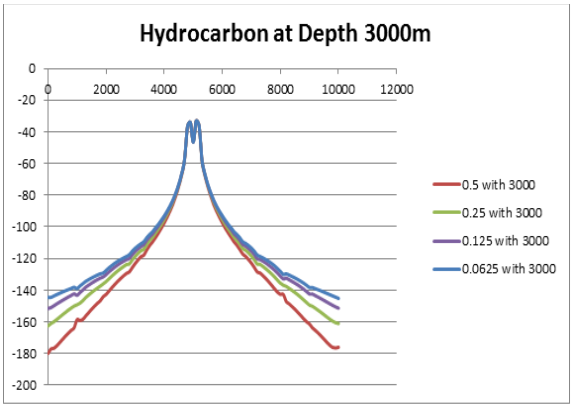

Figure 68: Magnitude of E-Field at Depth 2500m for Frequency 0.5Hz, 0.25Hz, 0.125Hz and 0.0625Hz (Excel)

DISCUSSION

From above observation, as the frequencies lower, the magnitude of the E-Field becomes higher. As the depth become deeper, the magnitude of E-Field becomes lower. This shows that frequencies are vice versa with the magnitude and E-Field and depth is proportional to E-Field. Furthermore, the graph looks similar to the graph produces by COMSOL software. Therefore, we can use the data to proceed with the next step which is looking for suitable trend line.

4.3 TRENDLINE FOR SEABED LOGGING (SBL)

For the experiment, the transmitter was placed at the center of model. For part 4.3, half part of the graph was taken. Logarithm trend line is added to the graph and result was shown below.

RESULT AT FREQUENCY 0.25Hz (Without Hydrocarbon)

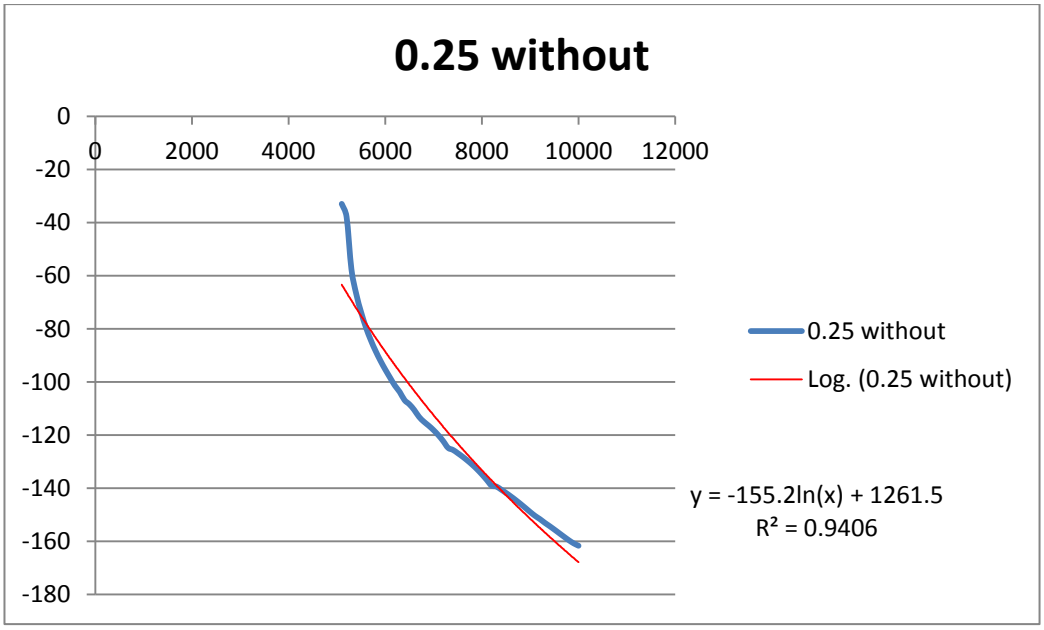

Figure 69: Comparison between Logarithm Graph and Actual Graph at Frequency 0.25Hz (Without Hydro)

RESULT AT FREQUENCY 0.25Hz (Depth 1000m)

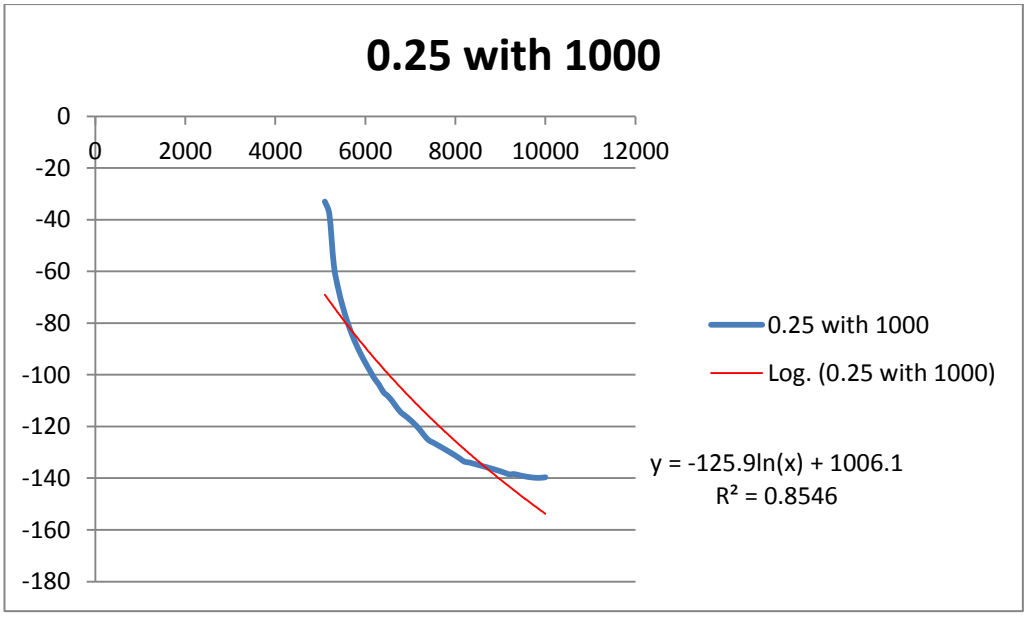

Figure 70: Comparison between Logarithm Graph and Actual Graph at Frequency 0.25Hz (Depth 1000m)

RESULT AT FREQUENCY 0.25Hz (Depth 1250m)

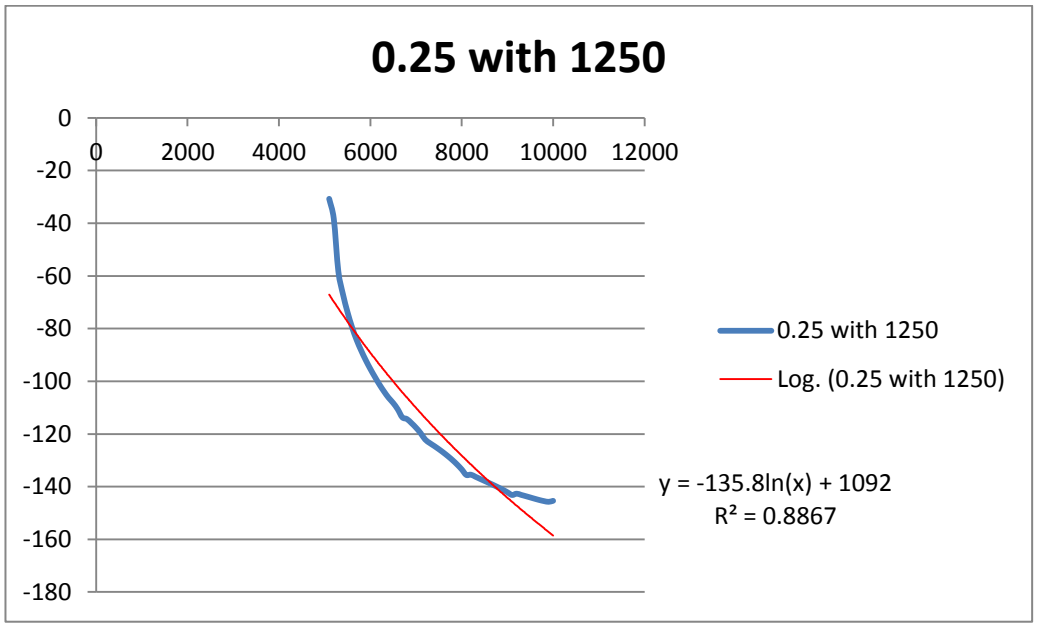

Figure 71: Comparison between Logarithm Graph and Actual Graph at Frequency 0.25Hz (Depth 1250m)

RESULT AT FREQUENCY 0.25Hz (Depth 1500m)

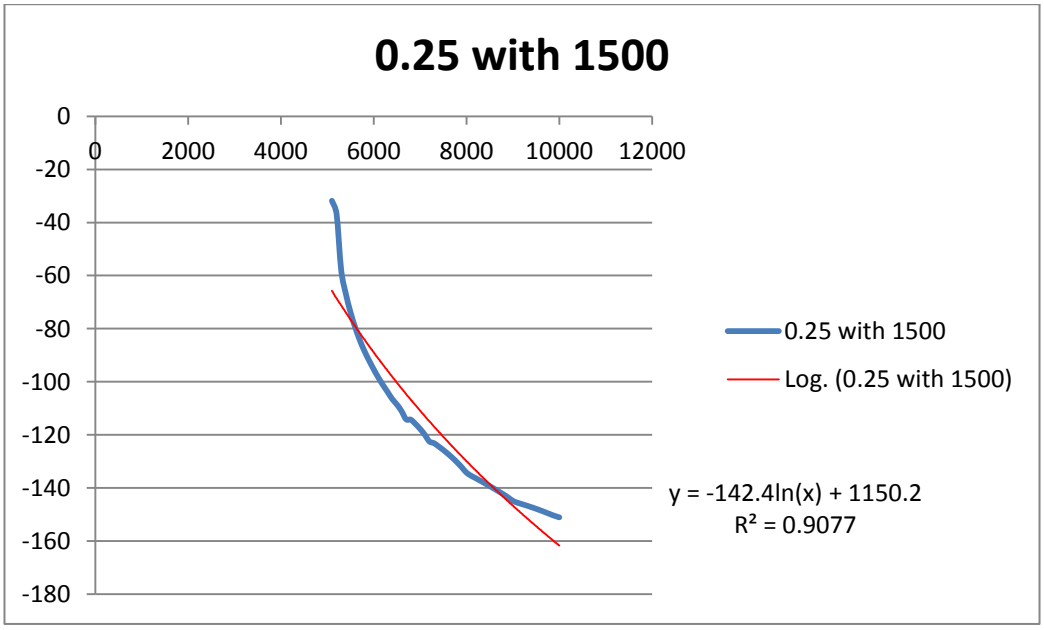

Figure 72: Comparison between Logarithm Graph and Actual Graph at Frequency 0.25Hz (Depth 1500m)

RESULT AT FREQUENCY 0.25Hz (Depth 1750m)

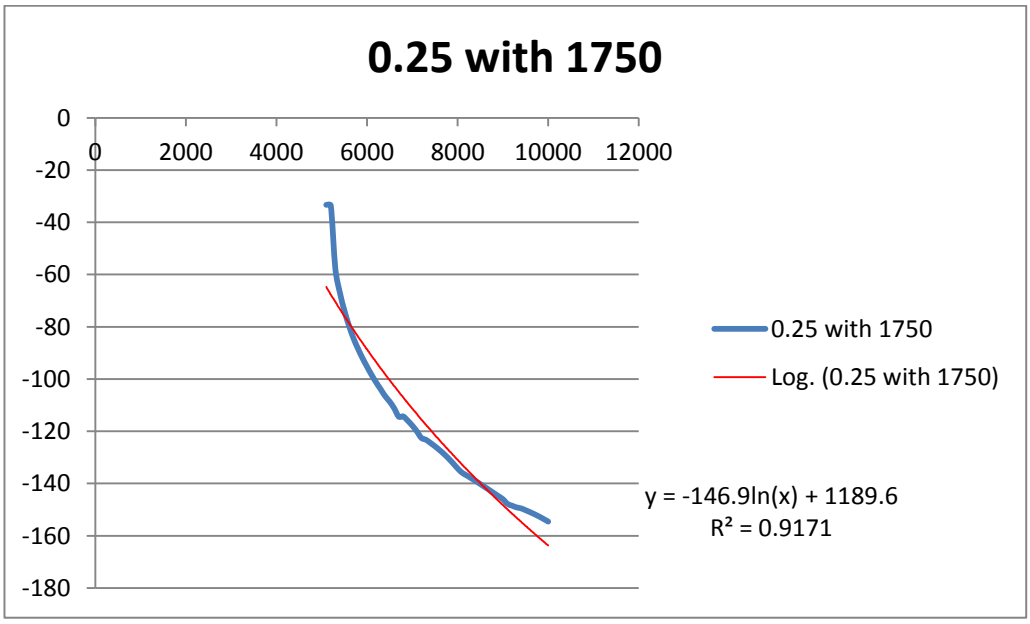

Figure 73: Comparison between Logarithm Graph and Actual Graph at Frequency 0.25Hz (Depth 1750m)

RESULT AT FREQUENCY 0.25Hz (Depth 2000m)

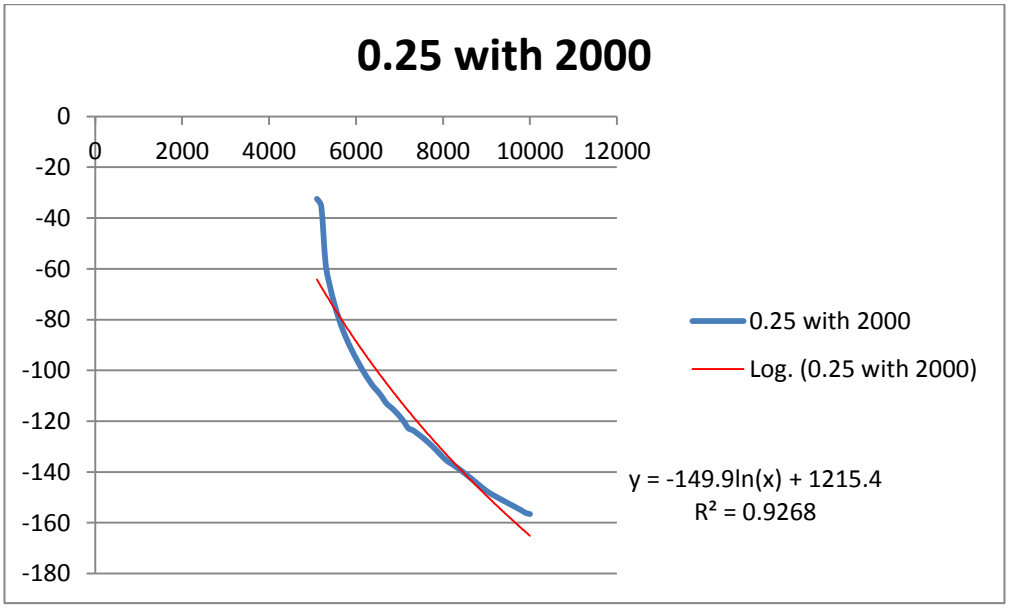

Figure 74: Comparison between Logarithm Graph and Actual Graph at Frequency 0.25Hz (Depth 2000m)

RESULT AT FREQUENCY 0.25Hz (Depth 2250m)

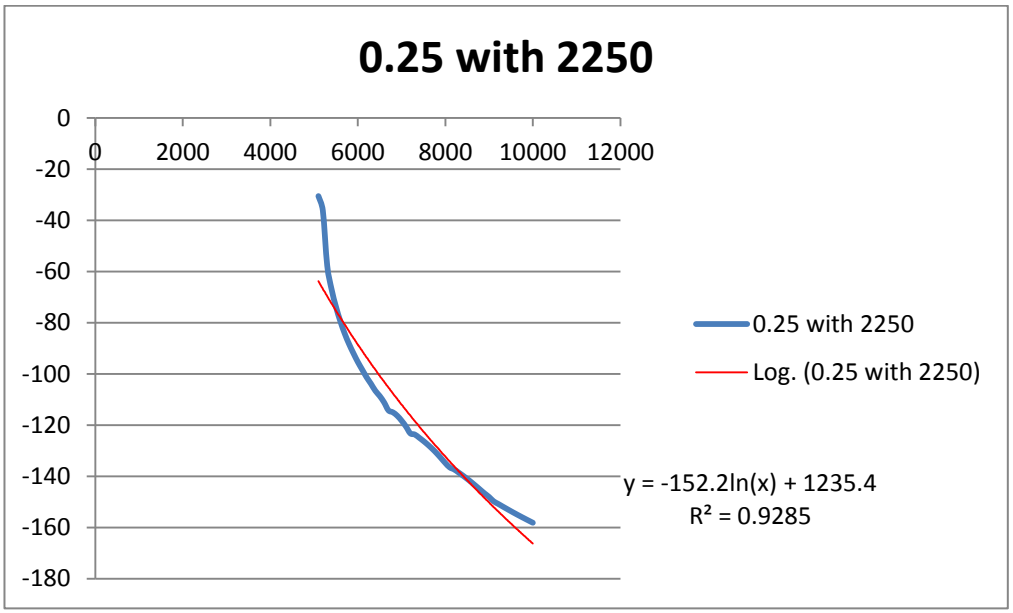

Figure 75: Comparison between Logarithm Graph and Actual Graph at Frequency 0.25Hz (Depth 2250m)

RESULT AT FREQUENCY 0.25Hz (Depth 2500m)

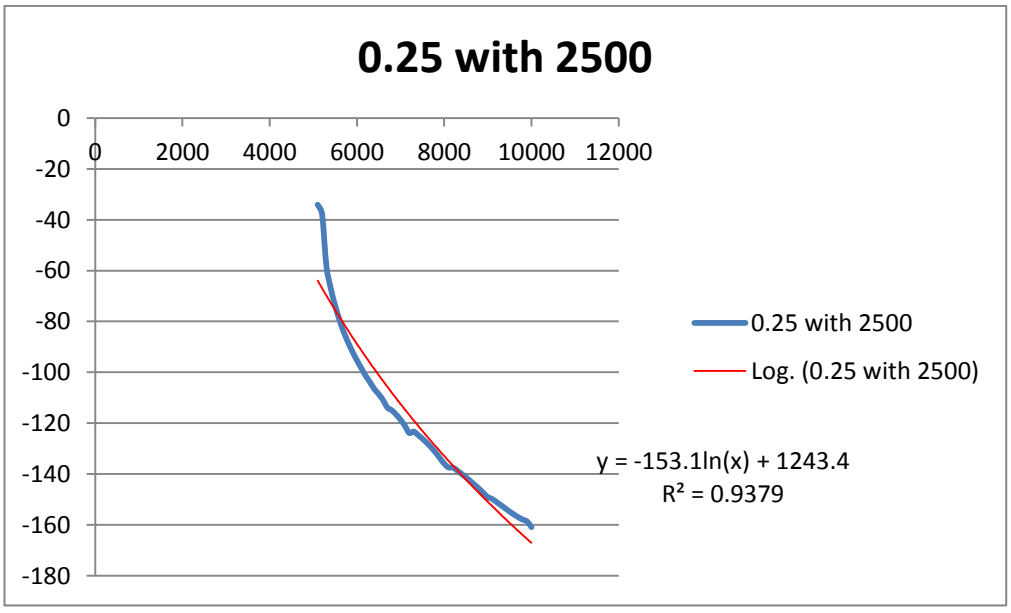

Figure 76: Comparison between Logarithm Graph and Actual Graph at Frequency 0.25Hz (Depth 2500m)

RESULT AT FREQUENCY 0.25Hz (Depth 2750m)

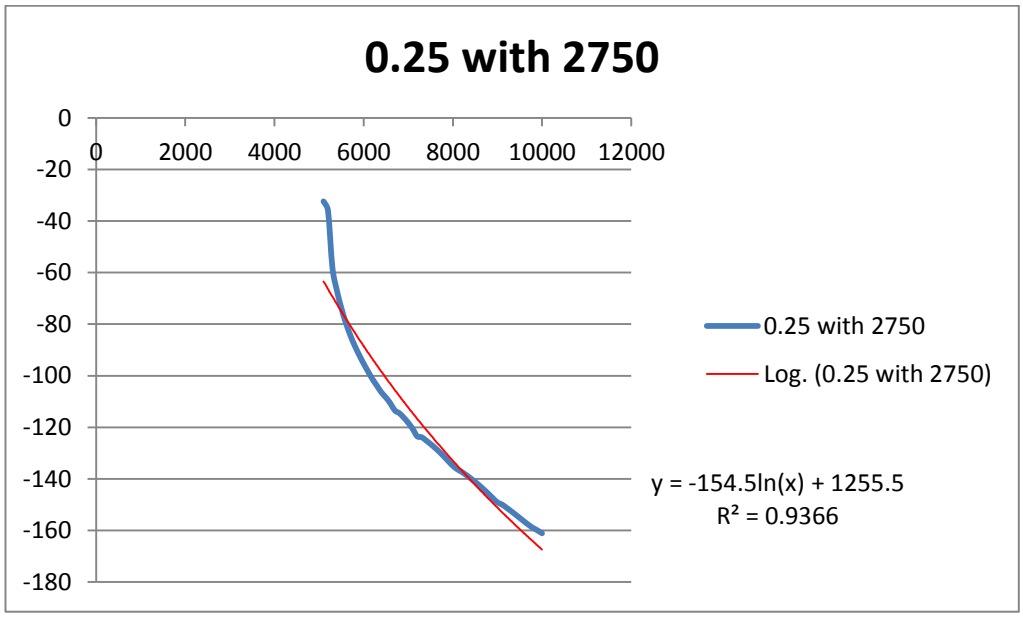

Figure 77: Comparison between Logarithm Graph and Actual Graph at Frequency 0.25Hz (Depth 2750m)

RESULT AT FREQUENCY 0.25Hz (Depth 3000m)

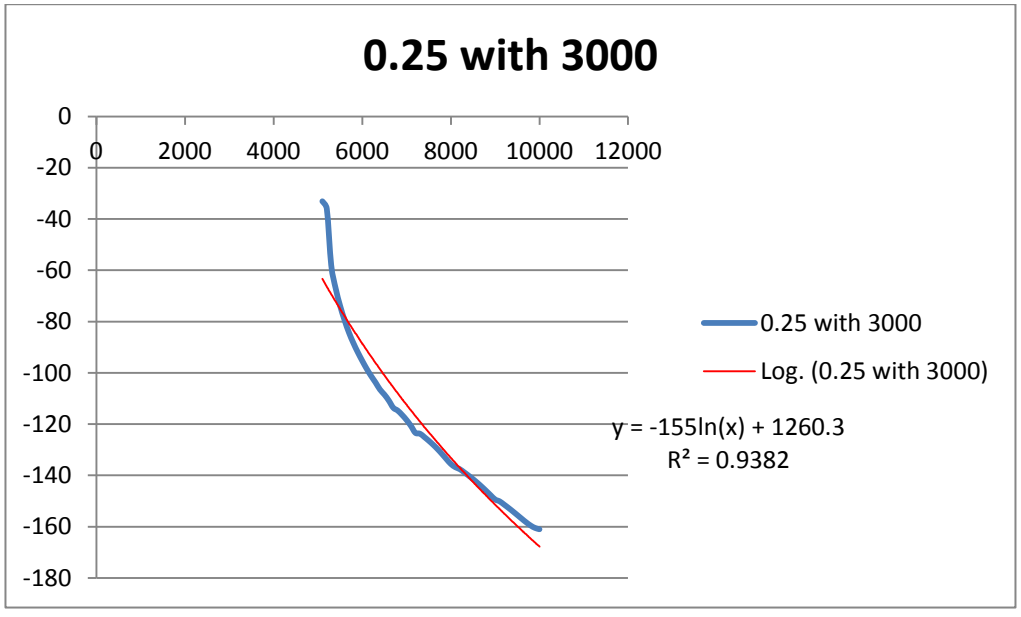

Figure 78: Comparison between Logarithm Graph and Actual Graph at Frequency 0.25Hz (Depth 3000m)

Table below shows the result for other frequencies as well as 0.25Hz frequency.

Table 7: Different between Logarithm Graph and Actual Graph

WITHOUT HYDRO				
FREQUENCIES	**0.5Hz**	**0.25Hz**	**0.125Hz**	**0.625Hz**
R^2	0.9636	0.9406	0.9215	0.9074
1000				
R^2	0.8711	0.8546	0.8485	0.857
Different	0.095994	0.091431	0.0792187	0.0555433
1250				
R^2	0.9097	0.8867	0.8708	0.8689
Different	0.055936	0.057304	0.055019	0.0424289
1500				
R^2	0.9348	0.9077	0.8878	0.88
Different	0.029888	0.034978	0.0365708	0.0301962
1750				
R^2	0.9461	0.9171	0.896	0.8851
Different	0.018161	0.024984	0.0276723	0.0245757
2000				
R^2	0.9556	0.9268	0.905	0.8923
Different	0.008302	0.014671	0.0179056	0.016641
2250				
R^2	0.9569	0.9285	0.9065	0.8928
Different	0.006953	0.012864	0.0162778	0.0160899
2500				
R^2	0.9626	0.9379	0.9176	0.9043
Different	0.001038	0.002871	0.0042322	0.0034164

2750				
R^2	0.9616	0.9366	0.9153	0.9007
Different	0.002076	0.004253	0.0067282	0.0073837
3000				
R^2	0.9618	0.9382	0.9179	0.9034
Different	0.001868	0.002552	0.0039067	0.0044082

DISCUSSION

Result was repeated for frequencies 0.25Hz, 0.125Hz and 0.0625Hz. R^2 is how well the trend line graph compares to the actual graph. Based on the observation, the value of R^2 is increasing until the depth is at 2500m and reduces a little at depth 2750m and 3000m for all frequencies. When comparing the R^2 for graph with and without hydrocarbon using equation

$$Different = \frac{R^2\ (without\ hydrocarbon) - R^2\ (with\ hydrocarbon)}{R^2\ (without\ hydrocarbon)}$$

It shows that the different is reduced until the depth is at 2500m. However, it increases a little for depth 2750m and 3000m.

4.4 COMPARISON BETWEEN TRENDLINE EXPRESSION AND MEASURED VALUE

For part 4.4, expression for trend line was used. Value for each offset was added to the expression and magnitude of E-Field for the expression and magnitude of E-Field from the experiment was compared and result was shown as below.

AT FREQUENCY 0.25Hz (Without Hydrocarbon)

Expression: y = -155.2ln(x) + 1261.5

Table 8: Comparison Magnitude of E-Field (Measured) and Magnitude of E-Field (Calculated) at Frequency 0.25Hz (Without Hydrocarbon)

Offset (m)	Magnitude of E-Field (Measured)	Magnitude E-Field (Calculated)	Percentage Error (%)	Distance from Transmitter (m)
5100	-32.9888	-63.4418	48.00137	100
5200	-37.8268	-66.4554	43.0794	200
5300	-57.525	-69.4117	17.12501	300
5400	-66.8634	-72.3127	7.535755	400
5500	-73.7155	-75.1605	1.92255	500
5600	-79.4482	-77.957	1.912836	600
5700	-84.2161	-80.704	4.351846	700
5800	-88.3388	-83.4032	5.917752	800
5900	-91.9902	-86.0562	6.895431	900
6000	-95.3133	-88.6647	7.498624	1000
6100	-98.3955	-91.23	7.854336	1100
6200	-101.398	-93.7537	8.153679	1200
6300	-103.795	-96.2369	7.853815	1300
6400	-106.867	-98.6811	8.294876	1400
6500	-108.43	-101.087	7.264075	1500
6600	-110.563	-103.457	6.868962	1600
6700	-113.16	-105.791	6.966045	1700
6800	-114.991	-108.09	6.384094	1800
6900	-116.482	-110.356	5.551192	1900
7000	-118.159	-112.589	4.947747	2000
7100	-120.078	-114.79	4.606016	2100
7200	-122.296	-116.961	4.56167	2200
7300	-124.818	-119.102	4.79954	2300

7400	-125.588	-121.213	3.609064	2400
7500	-126.821	-123.297	2.858827	2500
7600	-128.149	-125.352	2.231103	2600
7700	-129.588	-127.381	1.732584	2700
7800	-131.16	-129.384	1.373186	2800
7900	-132.892	-131.361	1.165385	2900
8000	-134.805	-133.313	1.119343	3000
8100	-136.894	-135.241	1.222579	3100
8200	-139.024	-137.145	1.370001	3200
8300	-139.39	-139.026	0.26139	3300
8400	-140.558	-140.885	0.232104	3400
8500	-141.793	-142.722	0.6506	3500
8600	-143.1	-144.537	0.99429	3600
8700	-144.481	-146.331	1.264582	3700
8800	-145.934	-148.105	1.466161	3800
8900	-147.444	-149.859	1.611385	3900
9000	-148.972	-151.593	1.729193	4000
9100	-150.425	-153.308	1.880621	4100
9200	-151.632	-155.004	2.17575	4200
9300	-153.01	-156.682	2.343388	4300
9400	-154.27	-158.342	2.57137	4400
9500	-155.582	-159.984	2.751525	4500
9600	-156.932	-161.609	2.894196	4600
9700	-158.29	-163.218	3.018877	4700
9800	-159.602	-164.809	3.159872	4800
9900	-160.775	-166.385	3.371553	4900
10000	-161.687	-167.945	3.725866	5000

AT FREQUENCY 0.25Hz (Depth 1000m)

Expression: y = -125.9ln(x) + 1006.1

Table 9: Comparison Magnitude of E-Field (Measured) and Magnitude of E-Field (Calculated) at Frequency 0.25Hz (Hydrocarbon at Depth 1000m)

Offset (m)	Magnitude of E-Field (Measured)	Magnitude E-Field (Calculated)	Percentage Error (%)	Distance from Transmitter (m)
5100	-32.9887	-68.7078	51.9869	100
5200	-37.8271	-71.1525	46.83661	200
5300	-57.5279	-73.5507	21.78474	300
5400	-66.872	-75.904	11.89928	400

5500	-73.7335	-78.2142	5.728679	500
5600	-79.4787	-80.4827	1.247498	600
5700	-84.2609	-82.7111	1.873762	700
5800	-88.3953	-84.9007	4.116067	800
5900	-92.0482	-87.0529	5.738269	900
6000	-95.3617	-89.1689	6.945014	1000
6100	-98.4157	-91.2499	7.85289	1100
6200	-101.383	-93.2971	8.66644	1200
6300	-103.711	-95.3116	8.812296	1300
6400	-106.667	-97.2943	9.63383	1400
6500	-108.247	-99.2463	9.068818	1500
6600	-110.251	-101.168	8.977485	1600
6700	-112.673	-103.062	9.325737	1700
6800	-114.722	-104.927	9.335578	1800
6900	-116.049	-106.765	8.696125	1900
7000	-117.516	-108.576	8.233564	2000
7100	-119.164	-110.362	7.975627	2100
7200	-121.053	-112.123	7.964517	2200
7300	-123.263	-113.86	8.258959	2300
7400	-125.22	-115.573	8.34775	2400
7500	-126.177	-117.263	7.602413	2500
7600	-127.151	-118.93	6.912139	2600
7700	-128.141	-120.576	6.27427	2700
7800	-129.152	-122.201	5.688408	2800
7900	-130.189	-123.804	5.157254	2900
8000	-131.265	-125.388	4.687364	3000
8100	-132.398	-126.952	4.289465	3100
8200	-133.608	-128.497	3.977445	3200
8300	-133.894	-130.023	2.977473	3300
8400	-134.366	-131.531	2.155376	3400
8500	-134.831	-133.021	1.361208	3500
8600	-135.298	-134.493	0.598715	3600
8700	-135.775	-135.949	0.127912	3700
8800	-136.269	-137.388	0.814467	3800
8900	-136.787	-138.81	1.457296	3900
9000	-137.337	-140.217	2.054136	4000
9100	-137.919	-141.608	2.6055	4100
9200	-138.527	-142.984	3.117027	4200
9300	-138.394	-144.345	4.123162	4300
9400	-138.78	-145.692	4.743904	4400
9500	-139.145	-147.024	5.359064	4500

9600	-139.467	-148.342	5.983109	4600
9700	-139.716	-149.647	6.636243	4700
9800	-139.855	-150.938	7.343248	4800
9900	-139.842	-152.217	8.129482	4900
10000	-139.647	-153.482	9.014019	5000

AT FREQUENCY 0.25Hz (Depth 1250m)

Expression: y = -135.8ln(x) + 1092

Table 10: Comparison Magnitude of E-Field (Measured) and Magnitude of E-Field (Calculated) at Frequency 0.25Hz (Hydrocarbon at Depth 1250m)

Offset (m)	Magnitude of E-Field (Measured)	Magnitude E-Field (Calculated)	Percentage Error (%)	Distance from Transmitter (m)
5100	-30.7357	-67.324	54.34661	100
5200	-38.2304	-69.961	45.35464	200
5300	-58.2392	-72.5478	19.72292	300
5400	-66.8528	-75.0861	10.96514	400
5500	-73.7075	-77.578	4.989072	500
5600	-79.4527	-80.0249	0.714987	600
5700	-84.3078	-82.4285	2.279935	700
5800	-88.3374	-84.7903	4.183469	800
5900	-91.9805	-87.1117	5.589155	900
6000	-95.3007	-89.3941	6.607415	1000
6100	-98.337	-91.6388	7.309404	1100
6200	-101.25	-93.847	7.888084	1200
6300	-103.882	-96.0198	8.188206	1300
6400	-106.255	-98.1584	8.248586	1400
6500	-108.229	-100.264	7.944058	1500
6600	-110.645	-102.337	8.11769	1600
6700	-113.689	-104.379	8.919213	1700
6800	-114.328	-106.391	7.459792	1800
6900	-115.866	-108.374	6.913343	1900
7000	-117.623	-110.328	6.612618	2000
7100	-119.673	-112.254	6.609508	2100
7200	-122.105	-114.153	6.965588	2200
7300	-123.443	-116.027	6.392089	2300
7400	-124.585	-117.874	5.693304	2400
7500	-125.794	-119.697	5.093653	2500
7600	-127.081	-121.496	4.596846	2600

7700	-128.461	-123.271	4.210222	2700
7800	-129.957	-125.023	3.946537	2800
7900	-131.604	-126.753	3.826676	2900
8000	-133.45	-128.461	3.883312	3000
8100	-135.567	-130.148	4.163332	3100
8200	-135.44	-131.815	2.750418	3200
8300	-136.241	-133.461	2.083562	3300
8400	-137.038	-135.087	1.444016	3400
8500	-137.832	-136.694	0.832273	3500
8600	-138.63	-138.282	0.251384	3600
8700	-139.443	-139.852	0.292823	3700
8800	-140.285	-141.404	0.791814	3800
8900	-141.174	-142.939	1.234916	3900
9000	-142.129	-144.456	1.610835	4000
9100	-143.167	-145.957	1.911497	4100
9200	-142.658	-147.441	3.244124	4200
9300	-143.121	-148.909	3.887045	4300
9400	-143.604	-150.362	4.494318	4400
9500	-144.102	-151.799	5.070124	4500
9600	-144.603	-153.221	5.624322	4600
9700	-145.079	-154.628	6.175319	4700
9800	-145.485	-156.021	6.752963	4800
9900	-145.753	-157.399	7.398973	4900
10000	-145.386	-158.764	8.426227	5000

AT FREQUENCY 0.25Hz (Depth 1500m)

Expression: y = -142.4ln(x) + 1150.2

Table 11: Comparison Magnitude of E-Field (Measured) and Magnitude of E-Field (Calculated) at Frequency 0.25Hz (Hydrocarbon at Depth 1500m)

Offset (m)	Magnitude of E-Field (Measured)	Magnitude E-Field (Calculated)	Percentage Error (%)	Distance from Transmitter (m)
5100	-31.8169	-65.4682	51.40091	100
5200	-36.7269	-68.2333	46.17453	200
5300	-57.9743	-70.9458	18.28366	300
5400	-66.8759	-73.6076	9.145276	400
5500	-73.7616	-76.2205	3.226025	500
5600	-79.4579	-78.7863	0.852414	600
5700	-84.2559	-81.3067	3.627261	700

5800	-88.373	-83.7833	5.477981	800
5900	-91.953	-86.2176	6.652226	900
6000	-95.2834	-88.6109	7.530092	1000
6100	-98.374	-90.9647	8.145287	1100
6200	-101.213	-93.2802	8.504292	1200
6300	-103.829	-95.5586	8.655259	1300
6400	-106.508	-97.8012	8.902638	1400
6500	-108.543	-100.009	8.533262	1500
6600	-111.036	-102.183	8.664058	1600
6700	-114.151	-104.324	9.419002	1700
6800	-114.256	-106.434	7.349194	1800
6900	-115.869	-108.513	6.778868	1900
7000	-117.725	-110.562	6.478455	2000
7100	-119.901	-112.582	6.500842	2100
7200	-122.461	-114.573	6.884031	2200
7300	-123.116	-116.538	5.644721	2300
7400	-124.357	-118.475	4.964809	2400
7500	-125.687	-120.387	4.402731	2500
7600	-127.12	-122.273	3.964371	2600
7700	-128.675	-124.134	3.658247	2700
7800	-130.373	-125.972	3.494262	2800
7900	-132.229	-127.786	3.477429	2900
8000	-134.222	-129.577	3.584631	3000
8100	-135.4	-131.346	3.087036	3100
8200	-136.326	-133.093	2.429331	3200
8300	-137.296	-134.819	1.837496	3300
8400	-138.282	-136.525	1.287244	3400
8500	-139.283	-138.21	0.776605	3500
8600	-140.303	-139.875	0.305857	3600
8700	-141.35	-141.522	0.121339	3700
8800	-142.438	-143.149	0.49661	3800
8900	-143.592	-144.758	0.805373	3900
9000	-144.849	-146.349	1.02524	4000
9100	-145.556	-147.923	1.599824	4100
9200	-146.099	-149.479	2.261129	4200
9300	-146.653	-151.018	2.890895	4300
9400	-147.227	-152.541	3.483835	4400
9500	-147.832	-154.048	4.035472	4500
9600	-148.472	-155.539	4.543591	4600
9700	-149.147	-157.015	5.010793	4700
9800	-149.84	-158.476	5.449025	4800

9900	-150.507	-159.921	5.886924	4900
10000	-151.06	-161.352	6.378743	5000

AT FREQUENCY 0.25Hz (Depth 1750m)

Expression: y = -146.9ln(x) + 1189.6

Table 12: Comparison Magnitude of E-Field (Measured) and Magnitude of E-Field (Calculated) at Frequency 0.25Hz (Hydrocarbon at Depth 1750m)

Offset (m)	Magnitude of E-Field (Measured)	Magnitude E-Field (Calculated)	Percentage Error (%)	Distance from Transmitter (m)
5100	-33.3167	-64.4847	48.33395	100
5200	-33.6337	-67.3372	50.05183	200
5300	-57.6161	-70.1354	17.85016	300
5400	-66.8406	-72.8813	8.288423	400
5500	-73.7621	-75.5767	2.401069	500
5600	-79.4667	-78.2237	1.589118	600
5700	-84.3591	-80.8237	4.374159	700
5800	-88.3415	-83.3786	5.952217	800
5900	-91.9793	-85.8898	7.090016	900
6000	-95.2645	-88.3587	7.815567	1000
6100	-98.3756	-90.7869	8.358864	1100
6200	-101.253	-93.1755	8.66913	1200
6300	-103.858	-95.526	8.722109	1300
6400	-106.535	-97.8394	8.887679	1400
6500	-108.62	-100.117	8.492738	1500
6600	-111.184	-102.36	8.621238	1600
6700	-114.393	-104.569	9.395087	1700
6800	-114.306	-106.745	7.082871	1800
6900	-115.942	-108.89	6.47644	1900
7000	-117.821	-111.003	6.141934	2000
7100	-120.01	-113.087	6.121998	2100
7200	-122.53	-115.142	6.416484	2200
7300	-123.231	-117.168	5.174272	2300
7400	-124.443	-119.167	4.427641	2400
7500	-125.747	-121.139	3.804301	2500
7600	-127.16	-123.084	3.311268	2600
7700	-128.702	-125.005	2.958174	2700
7800	-130.396	-126.9	2.754931	2800
7900	-132.251	-128.771	2.701831	2900

8000	-134.218	-130.619	2.755318	3000
8100	-135.867	-132.444	2.584291	3100
8200	-136.901	-134.247	1.977458	3200
8300	-137.967	-136.027	1.426248	3300
8400	-139.062	-137.786	0.925826	3400
8500	-140.182	-139.525	0.470893	3500
8600	-141.322	-141.243	0.05584	3600
8700	-142.477	-142.941	0.324896	3700
8800	-143.642	-144.62	0.676339	3800
8900	-144.814	-146.28	1.002633	3900
9000	-145.987	-147.922	1.307652	4000
9100	-147.764	-149.545	1.190859	4100
9200	-148.457	-151.15	1.781568	4200
9300	-149.126	-152.738	2.365106	4300
9400	-149.488	-154.31	3.124503	4400
9500	-150.208	-155.864	3.628819	4500
9600	-150.959	-157.402	4.093622	4600
9700	-151.759	-158.925	4.508937	4700
9800	-152.625	-160.431	4.865634	4800
9900	-153.568	-161.923	5.159346	4900
10000	-154.576	-163.399	5.399627	5000

AT FREQUENCY 0.25Hz (Depth 2000m)

Expression: y = -149.9ln(x) + 1215.4

Table 13: Comparison Magnitude of E-Field (Measured) and Magnitude of E-Field (Calculated) at Frequency 0.25Hz (Hydrocarbon at Depth 2000m)

Offset (m)	Magnitude of E-Field (Measured)	Magnitude E-Field (Calculated)	Percentage Error (%)	Distance from Transmitter (m)
5100	-32.4523	-64.2957	49.5264	100
5200	-35.4575	-67.2064	47.24093	200
5300	-58.0542	-70.0618	17.13849	300
5400	-66.8926	-72.8637	8.19489	400
5500	-73.7763	-75.6143	2.430693	500
5600	-79.44	-78.3152	1.436146	600
5700	-84.274	-80.9684	4.082556	700
5800	-88.3351	-83.5754	5.695108	800
5900	-91.9533	-86.1379	6.751258	900
6000	-95.279	-88.6573	7.468954	1000

6100	-98.3927	-91.135	7.963697	1100
6200	-101.353	-93.5725	8.315277	1200
6300	-103.956	-95.9709	8.320782	1300
6400	-106.402	-98.3316	8.207339	1400
6500	-108.296	-100.656	7.590904	1500
6600	-110.521	-102.944	7.359854	1600
6700	-113.062	-105.198	7.474894	1700
6800	-114.505	-107.419	6.596594	1800
6900	-116.138	-109.608	5.957748	1900
7000	-118.013	-111.764	5.591268	2000
7100	-120.207	-113.891	5.545477	2100
7200	-122.766	-115.987	5.844712	2200
7300	-123.517	-118.055	4.626697	2300
7400	-124.734	-120.094	3.863385	2400
7500	-126.041	-122.106	3.222033	2500
7600	-127.451	-124.092	2.706908	2600
7700	-128.979	-126.051	2.322591	2700
7800	-130.634	-127.986	2.069484	2800
7900	-132.403	-129.895	1.930232	2900
8000	-134.196	-131.781	1.833017	3000
8100	-135.75	-133.643	1.576832	3100
8200	-136.832	-135.482	0.996271	3200
8300	-138.013	-137.299	0.519658	3300
8400	-139.252	-139.094	0.113117	3400
8500	-140.549	-140.868	0.226502	3500
8600	-141.902	-142.622	0.50451	3600
8700	-143.301	-144.355	0.730238	3700
8800	-144.724	-146.068	0.920227	3800
8900	-146.131	-147.762	1.103413	3900
9000	-147.451	-149.436	1.328331	4000
9100	-148.567	-151.093	1.671558	4100
9200	-149.527	-152.731	2.097826	4200
9300	-150.476	-154.352	2.510944	4300
9400	-151.41	-155.955	2.914502	4400
9500	-152.328	-157.541	3.309115	4500
9600	-153.238	-159.111	3.691229	4600
9700	-154.154	-160.664	4.052301	4700
9800	-155.099	-162.202	4.37866	4800
9900	-156.107	-163.723	4.65234	4900
10000	-156.574	-165.23	5.238701	5000

AT FREQUENCY 0.25Hz (Depth 2250m)

Expression: y = -152.2ln(x) + 1235.4

Table 14: Comparison Magnitude of E-Field (Measured) and Magnitude of E-Field (Calculated) at Frequency 0.25Hz (Hydrocarbon at Depth 2250m)

Offset (m)	Magnitude of E-Field (Measured)	Magnitude E-Field (Calculated)	Percentage Error (%)	Distance from Transmitter (m)
5100	-30.5653	-63.9308	52.19003	100
5200	-36.1733	-66.8862	45.91819	200
5300	-57.6691	-69.7853	17.36208	300
5400	-66.943	-72.6303	7.830398	400
5500	-73.7469	-75.423	2.222284	500
5600	-79.4132	-78.1654	1.596333	600
5700	-84.2405	-80.8593	4.181531	700
5800	-88.3515	-83.5063	5.80212	800
5900	-91.9625	-86.1081	6.798949	900
6000	-95.3429	-88.6661	7.53023	1000
6100	-98.3413	-91.1819	7.851731	1100
6200	-101.302	-93.6568	8.162553	1200
6300	-103.863	-96.092	8.086862	1300
6400	-106.596	-98.4889	8.231553	1400
6500	-108.63	-100.849	7.716171	1500
6600	-111.125	-103.172	7.707924	1600
6700	-114.25	-105.461	8.333893	1700
6800	-115.007	-107.716	6.769182	1800
6900	-116.337	-109.938	5.820763	1900
7000	-118.273	-112.128	5.480655	2000
7100	-120.55	-114.287	5.480232	2100
7200	-123.239	-116.415	5.86138	2200
7300	-123.674	-118.515	4.353407	2300
7400	-124.902	-120.586	3.579138	2400
7500	-126.227	-122.629	2.934168	2500
7600	-127.668	-124.645	2.425783	2600
7700	-129.247	-126.634	2.063271	2700
7800	-130.982	-128.598	1.854025	2800
7900	-132.872	-130.537	1.789061	2900
8000	-134.831	-132.451	1.796792	3000
8100	-136.533	-134.342	1.63121	3100
8200	-137.316	-136.21	0.812237	3200
8300	-138.484	-138.054	0.311291	3300

8400	-139.716	-139.877	0.114956	3400
8500	-141.016	-141.678	0.467737	3500
8600	-142.382	-143.459	0.750117	3600
8700	-143.81	-145.218	0.969518	3700
8800	-145.278	-146.958	1.142855	3800
8900	-146.735	-148.677	1.306244	3900
9000	-148.077	-150.378	1.529903	4000
9100	-149.715	-152.06	1.541831	4100
9200	-150.702	-153.723	1.965063	4200
9300	-151.691	-155.369	2.366862	4300
9400	-152.673	-156.996	2.753899	4400
9500	-153.639	-158.607	3.132432	4500
9600	-154.582	-160.201	3.507301	4600
9700	-155.5	-161.778	3.880793	4700
9800	-156.394	-163.339	4.251806	4800
9900	-157.273	-164.884	4.615864	4900
10000	-158.149	-166.414	4.966657	5000

AT FREQUENCY 0.25Hz (Depth 2500m)

Expression: y = -153.1ln(x) + 1243.4

Table 15: Comparison Magnitude of E-Field (Measured) and Magnitude of E-Field (Calculated) at Frequency 0.25Hz (Hydrocarbon at Depth 2500m)

Offset (m)	Magnitude of E-Field (Measured)	Magnitude E-Field (Calculated)	Percentage Error (%)	Distance from Transmitter (m)
5100	-34.1001	-63.6141	46.39539	100
5200	-37.7019	-66.587	43.37943	200
5300	-58.1877	-69.5032	16.2806	300
5400	-66.976	-72.365	7.446927	400
5500	-73.7499	-75.1743	1.894697	500
5600	-79.42	-77.9329	1.908123	600
5700	-84.2571	-80.6427	4.482009	700
5800	-88.3272	-83.3054	6.028172	800
5900	-91.9676	-85.9225	7.035438	900
6000	-95.305	-88.4957	7.694478	1000
6100	-98.3591	-91.0263	8.055596	1100
6200	-101.348	-93.5158	8.374976	1200
6300	-103.878	-95.9655	8.245158	1300
6400	-106.612	-98.3766	8.371723	1400

6500	-108.582	-100.75	7.773031	1500
6600	-110.97	-103.088	7.645985	1600
6700	-113.917	-105.39	8.090657	1700
6800	-114.923	-107.658	6.747993	1800
6900	-116.653	-109.893	6.151026	1900
7000	-118.661	-112.096	5.85652	2000
7100	-121.043	-114.268	5.929493	2100
7200	-123.868	-116.409	6.407782	2200
7300	-123.295	-118.521	4.028073	2300
7400	-124.628	-120.604	3.336204	2400
7500	-126.082	-122.659	2.790769	2500
7600	-127.686	-124.687	2.40515	2600
7700	-129.471	-126.688	2.196749	2700
7800	-131.47	-128.664	2.18094	2800
7900	-133.674	-130.614	2.342442	2900
8000	-135.892	-132.54	2.5289	3000
8100	-137.419	-134.442	2.214496	3100
8200	-137.43	-136.32	0.813882	3200
8300	-138.649	-138.176	0.342579	3300
8400	-139.94	-140.01	0.049592	3400
8500	-141.306	-141.821	0.363639	3500
8600	-142.746	-143.612	0.602785	3600
8700	-144.255	-145.382	0.775514	3700
8800	-145.761	-147.132	0.931498	3800
8900	-147.458	-148.862	0.94278	3900
9000	-149.055	-150.572	1.007998	4000
9100	-149.782	-152.264	1.629863	4100
9200	-150.999	-153.937	1.908947	4200
9300	-152.245	-155.593	2.151556	4300
9400	-153.501	-157.23	2.371363	4400
9500	-154.739	-158.85	2.588108	4500
9600	-155.916	-160.453	2.827848	4600
9700	-156.983	-162.04	3.120536	4700
9800	-157.894	-163.61	3.493845	4800
9900	-158.616	-165.164	3.964879	4900
10000	-160.884	-166.703	3.490614	5000

AT FREQUENCY 0.25Hz (Depth 2750m)

Expression: y = -154.5ln(x) + 1255.5

Table 16: Comparison Magnitude of E-Field (Measured) and Magnitude of E-Field (Calculated) at Frequency 0.25Hz (Hydrocarbon at Depth 2750m)

Offset (m)	Magnitude of E-Field (Measured)	Magnitude E-Field (Calculated)	Percentage Error (%)	Distance from Transmitter (m)
5100	-32.3921	-63.4659	48.96138	100
5200	-35.9279	-66.4659	45.94536	200
5300	-58.1742	-69.4089	16.18629	300
5400	-66.9522	-72.2968	7.392628	400
5500	-73.7738	-75.1318	1.807449	500
5600	-79.4606	-77.9156	1.982859	600
5700	-84.2744	-80.6502	4.49375	700
5800	-88.3618	-83.3372	6.029186	800
5900	-91.9721	-85.9783	6.971251	900
6000	-95.3118	-88.575	7.605759	1000
6100	-98.4119	-91.1288	7.992142	1100
6200	-101.375	-93.6411	8.258664	1200
6300	-103.951	-96.1131	8.155257	1300
6400	-106.512	-98.5462	8.083001	1400
6500	-108.45	-100.942	7.438669	1500
6600	-110.762	-103.3	7.223138	1600
6700	-113.481	-105.624	7.439134	1700
6800	-114.531	-107.913	6.132574	1800
6900	-116.252	-110.168	5.522139	1900
7000	-118.26	-112.391	5.221528	2000
7100	-120.652	-114.583	5.297123	2100
7200	-123.491	-116.744	5.779972	2200
7300	-123.834	-118.875	4.171797	2300
7400	-125.106	-120.977	3.41288	2400
7500	-126.475	-123.051	2.782834	2500
7600	-127.957	-125.097	2.286217	2600
7700	-129.566	-127.117	1.926893	2700
7800	-131.306	-129.11	1.700982	2800
7900	-133.144	-131.078	1.57595	2900
8000	-134.934	-133.022	1.437251	3000
8100	-136.295	-134.941	1.003355	3100
8200	-137.29	-136.837	0.330881	3200
8300	-138.505	-138.71	0.147777	3300

8400	-139.795	-140.56	0.544321	3400
8500	-141.168	-142.388	0.857402	3500
8600	-142.629	-144.195	1.08621	3600
8700	-144.182	-145.982	1.232426	3700
8800	-145.819	-147.747	1.305023	3800
8900	-147.503	-149.493	1.331527	3900
9000	-149.13	-151.219	1.381381	4000
9100	-149.914	-152.927	1.969809	4100
9200	-151.142	-154.615	2.246345	4200
9300	-152.428	-156.285	2.468134	4300
9400	-153.766	-157.938	2.64131	4400
9500	-155.14	-159.573	2.777601	4500
9600	-156.519	-161.191	2.898018	4600
9700	-157.847	-162.792	3.037334	4700
9800	-159.039	-164.376	3.246707	4800
9900	-159.991	-165.945	3.588105	4900
10000	-161.102	-167.498	3.818198	5000

AT FREQUENCY 0.25Hz (Depth 3000m)

Expression: y = -155ln(x) + 1260.3

Table 17: Comparison Magnitude of E-Field (Measured) and Magnitude of E-Field (Calculated) at Frequency 0.25Hz (Hydrocarbon at Depth 3000m)

Offset (m)	Magnitude of E-Field (Measured)	Magnitude E-Field (Calculated)	Percentage Error (%)	Distance from Transmitter (m)
5100	-33.0913	-62.9344	47.41929	100
5200	-35.9545	-65.9442	45.47736	200
5300	-57.9868	-68.8966	15.83514	300
5400	-67.0212	-71.7939	6.647758	400
5500	-73.7894	-74.638	1.137002	500
5600	-79.388	-77.4309	2.527557	600
5700	-84.2897	-80.1743	5.133094	700
5800	-88.3686	-82.87	6.635167	800
5900	-91.9787	-85.5197	7.552725	900
6000	-95.2888	-88.1248	8.129378	1000
6100	-98.3984	-90.6868	8.503509	1100
6200	-101.206	-93.2072	8.582089	1200
6300	-103.757	-95.6873	8.433522	1300
6400	-106.505	-98.1283	8.536413	1400

6500	-108.468	-100.531	7.894334	1500
6600	-110.82	-102.898	7.698863	1600
6700	-113.608	-105.229	7.962952	1700
6800	-114.714	-107.525	6.685635	1800
6900	-116.417	-109.788	6.037891	1900
7000	-118.393	-112.018	5.690607	2000
7100	-120.721	-114.217	5.694464	2100
7200	-123.415	-116.385	6.040741	2200
7300	-123.7	-118.523	4.368307	2300
7400	-125.023	-120.631	3.640202	2400
7500	-126.458	-122.712	3.052654	2500
7600	-128.026	-124.765	2.613794	2600
7700	-129.748	-126.791	2.331763	2700
7800	-131.632	-128.791	2.205446	2800
7900	-133.634	-130.766	2.193609	2900
8000	-135.542	-132.716	2.129838	3000
8100	-136.797	-134.641	1.60101	3100
8200	-137.561	-136.543	0.745972	3200
8300	-138.781	-138.422	0.259317	3300
8400	-140.073	-140.278	0.14587	3400
8500	-141.447	-142.112	0.468427	3500
8600	-142.907	-143.925	0.707613	3600
8700	-144.457	-145.717	0.864948	3700
8800	-146.089	-147.489	0.948947	3800
8900	-147.768	-149.24	0.986631	3900
9000	-149.389	-150.972	1.048408	4000
9100	-150.114	-152.685	1.683586	4100
9200	-151.357	-154.379	1.957199	4200
9300	-152.667	-156.054	2.170521	4300
9400	-154.04	-157.712	2.328094	4400
9500	-155.464	-159.352	2.440341	4500
9600	-156.905	-160.975	2.528627	4600
9700	-158.301	-162.582	2.632702	4700
9800	-159.546	-164.171	2.817527	4800
9900	-160.493	-165.745	3.168422	4900
10000	-161.013	-167.303	3.759683	5000

DISCUSSION:

From the table above, the error between measured graph and calculated graph is quiet small which is less than 10%. It shows that the expression can be used to determine the location of the hydrocarbon. Different depth has different expression and percentage error between the measured graph and calculated graph is shown as below:

$$Percentage\ Error\ (\%) = \left|\frac{Calculated\ Value - Measured\ Value}{Calulated\ Value}\right| \text{x } 100\%$$

CHAPTER 5
CONCLUSION

To summarize for first of the experiment where same frequency is used for different depth, as the depth of the hydrocarbon location from the seafloor increases, the magnitude of E-Field will reduce until a certain point, where the frequency with and without hydrocarbon is equal, the frequency is no longer suitable to locate the hydrocarbon.

For second of the experiment where the depth is fixed and the frequency is varied, as lower as the frequency, wavelength will increase and magnitude of E-Field will be higher.

For third part where the expression for each depth and frequency were generated, it is important as by using the expression, time to locate the hydrocarbon can be shorten. For example, frequency of the transmitter can be set. Then as receiver recorded the data, the data will be added with a trend line and compared with the graph generated by the simulator. Location of the hydrocarbon can be determined by nearest value of trend line for the specific depth.

In a nutshell, the project will bring lots of advantages and benefits in the future especially for oil and gas industry in searching for hydrocarbon particularly in deep water. From the 3D model for seabed logging, the data gathered was analyzed in FYP2 and forward mathematical models generated from the synthesis data. The data contain at the receivers are huge and with the forward mathematical model, author believe that all the difficulty to interpret the data can be improve. Furthermore, in searching for hydrocarbon underneath the seabed, the forward mathematical models are expect to reduce the cost and time to search the hydrocarbon.

REFERENCES

[1] Dyke Kate Van, "Fundamentals of Petroleum" Texas: Petroleum Extension Services, 1997. - Vol. Fourth Edition.

[2] http://www.ngi.no/en/Selected-topics/EM-technology-in-ocean-depths/NGI-and-Statoil-announced-EM-boom

[3] Minerals & Petroleum Resources Directorate (2007) "A Citizen's Guide for the Northwest Territories", July 20, 2010.

[4] http://www.enviroscan .com/html/seismic_refraction_versus_refl.html

[5] M. Ray Tomasson and Larry Nation "MT Gauges Earth's Electric Fields" in Geophysical Corner, AAPG Explorer, December 1998 and "MT Data Throws Curves to Viewers", in Geophysical Corner, AAPG Explorer, January 1999.

[6] Dr. David George Peace and Arnold Orange "Marine MT & Controlled Source Electro-Magnetics for Hydrocarbon Exploration".

[7] Steven C. Constable, Arnold S. Orangez, G. Michael Hoversten and H. Frank Morrison "Marine Magnetotellurics for Petroleum Exploration Part 1: A Sea-Floor Equipment System".

[8] Arnold S. Orange "Magnetotelluric Exploration for Hydrocarbons".

[9] Steven Constable "Ten Years of marine CSEM for Hydrocarbon Exploration", Geophysics, Vol. 75, No. 5, September-October 2010.

[10] Martyn Unsworth "New Developments in Conventional Hydrocarbon Exploration with Electromagnetic Methods", Department of Physics and Institute for Geophysical Research, University of Alberta, Edmonton, Alberta, Canada.

[11] B.P. Lindom, J.E. Lie and D. Ridyard, EMGS Americas "Electromagnetic Prospect Scanning- Seabed Logging Moves from Risk Reduction to Value Creation", Society of Petroleum Engineering.

[12] T. Eidesmo, S. Ellingsrud, L.M. MacGregor, S. Constable, M.C. sinha, S. Johansen, F.N. Kong and H. Westerdahl "Sea Bed Logging (SBL), a New Method for Remote and Direct Identification of hydrocarbon Filled Layers in Deepwater Areas".

[13] http://www/sciencedirect.com

[14] M.R.Islam Enhanced Oil Recovery of Ugnu Tar Sands of Alaska Using Electromagnetic Heating with Horizontal Wells, , EMERTEC Developments Inc. and S.S Wadader and A.Bansal, U.of Alaska Fairbanks

[15] Julius Adams Stratton A Classic Reissue Electromagnetic Theory, The IEEE Press Series on Electromagnetic Wave Theory, Donald G. Dudley, Series Editor pg. 2

[16] Electromagnetic Field Theory First Edition 2009 U.A. Bakshi and A.V. Bakshi, Technical Publication Pune TM pg 7-4, 7-47

[17] Steven Constabler "GC Marine EM Methods", October 32, 2005

[18] College Physics Volume 2: Chapter 15-30 Raymond A. Serway Jerry S. Faughn and Chris Vuille pg. 715-716

[19] L.-J. Gelius, "Multi-component Processing of Sea Bed Logging Data", Department of Geoscience, University of Oslo, Norway, PIERS ONLINE, Vol. 2, No 6, 2006

[20] Ulaby Fawwaz T. "Electromagnetics for Engineers". New Jersey : Pearson Education, 2005.

[21] Umran S. Inan and Robert A. Marshall "Numerical Electromagnetic, The FDTD Method", New York: Cambridge University Press, 2011.

[22] Bahaa Saleh "Introduction to Subsurface Imaging", New York: Cambridge University Press, 2011.